"In presenting the dissertation as a partial fulfillment of the requirements for an advanced degree from the Georgia Institute of Technology, I agree that the Library of the Institution shall make it available for inspection and circulation in accordance with its regulations governing materials of this type. I agree that permission to copy from, or to publish from, this dissertation may be granted by the professor under whose direction it was written, or, in his absence, by the dean of the Graduate Division when such copying or publication is solely for scholarly purposes and does not involve potential financial gain. It is understood that any copying from, or publication of, this dissertation which involves potential financial gain will not be allowed without written permission.

_____"

MOMENTUM AND HEAT TRANSFER TO A FLUID FLOWING TURBULENTLY IN A PIPE

A THESIS

Presented to

the Faculty of the Graduate Division

by

Robert James Hefner

In Partial Fulfillment

of the Requirements for the Degree

Doctor of Philosophy

in the School of Chemical Engineering

Georgia Institute of Technology

October 1959

12R
7a

MOMENTUM AND HEAT TRANSFER TO A FLUID FLOWING TURBULENTLY IN A PIPE

Approved:

William B. Harrison, III,
Thesis Advisor

Henderson C. Ward

William Meese Newton

Date Approved by Chairman: October 25, 1959

ACKNOWLEDGEMENTS

The author wishes to express his appreciation to those who gave invaluable assistance in the course of this investigation: to the late Dr. J. M. DallaValle who gave indispensable advice and guidance throughout his academic career, to Dr. W. B. Harrison for his advice and cheerful guidance and to the kind people associated with the Rich Computer Center and School of Chemical Engineering.

The author is also grateful to the Shell Oil Company for the Shell Fellowship in Chemical Engineering during the academic years of 1956-57 and 1957-58.

The author's gratitude to his wife and daughters is immeasurable.

TABLE OF CONTENTS

LIST OF SYMBOLS

A	Surface area, $2\pi R\Delta x$	ft^2
C_P	Specific heat at constant pressure	$Btu/lb_m\ °F$
D	Diameter of pipe	ft
f	Friction factor, $8g_c\ \tau_w/\rho u^2$	
g_c	Conversion factor	$ft\ lb_m/hr^2\ lb_f$
h	Coefficient of heat transfer between fluid and surface	$Btu/hr\ ft^2$
k	Thermal conductivity of fluid	$Btu/hr\ ft^2\ °F/ft$
Nu	Nusselt number, hD/k	
P	Pressure	lb_f/ft^2
Pe	Peclet number, Re Pr	
Pr	Prandtl number, ν/α	
q	Heat transfer rate	Btu/hr
Re	Reynolds number, Du/ν	
Re*	"Friction velocity" Reynolds number, Du^*/ν	
r	Radial distance from pipe center	ft
R	Radius of pipe	ft
R^+	Radius of pipe in dimensionless form, $1/2\ Re\ \sqrt{f/8}$	
S	Parameter, $q_w/A_w\rho C_P$	$°F\ ft/sec$
t	Temperature of fluid at any point	°F
u	Axial velocity component	ft/hr
u^+	Dimensionless velocity, $\bar{u}\ \sqrt{g_c\ \tau_w/\rho}$	

u^*	Friction velocity, $\sqrt{g_c \tau_w/\rho}$	ft/hr
w	Radial distance from pipe wall divided by radius of pipe, y/R	
x	Distance in axial direction	ft
y	Radial distance from pipe wall, R-r	ft
y^+	Radial distance from pipe wall in dimensionless form, $\sqrt{g_c \tau_w/\rho}\ y/\nu$	
z	Radial distance from pipe wall divided by radius of pipe, y/R	

Greek Letters

α	Thermal diffusivity of fluid	ft^2/hr
ϵ_H	Eddy diffusivity of heat transfer	ft^2/hr
ϵ_m	Eddy diffusivity of momentum-transfer	ft^2/hr
θ	Temperature at pipe wall minus temperature at any point, $t_w - \bar{t}$	°F
λ	Parameter, $\sqrt{f/8}$	
ν	Kinematic viscosity of fluid	ft^2/hr
ρ	Density of fluid	lb_m/ft^3
σ	Ratio of eddy diffusivities of heat and momentum	
τ	Shear stress at any point	lb_f/ft^2

Subscripts

c	Quantity measured at pipe center
m	Bulk mean
r	Local radius at a point
w	Quantity measured at pipe wall

Superscripts

'	Fluctuating component
-	Temporal mean

LIST OF TABLES

LIST OF FIGURES

SUMMARY

Techniques utilizing analogy methods for the calculation of heat transfer coefficients for the turbulent flow of fluids in round pipe have been presented by several investigators during the past decade. The majority of these investigations have been conducted for fluids such as liquid metals which exhibit Prandtl numbers considerably less than unity. It was the purpose of this investigation to study momentum-heat transfer analogy methods for the prediction of heat transfer coefficients for the complete range of fluids.

The majority of the momentum-heat transfer analogy models presented to date have been based upon the use of the universal dimensionless velocity distribution equations of von Karman (Transactions of the American Society of Mechanical Engineers, 61, 705-710, 1939). A large portion of the discrepancy existing between the experimental data for fluids with Prandtl numbers of the order of magnitude one or greater and the predictions of the analogy models based on the von Karman equations can be attributed to the inaccuracy of these equations in the region very close to the pipe wall. Also, since the velocity gradient expressed by the von Karman equations is not a continuous function across the entire region of flow within the pipe, models employing these equations must contain additional assumptions as to the state of flow and relative magnitudes of the molecular and eddy diffusivities of momentum and heat within the various regions of flow within the pipe.

In order to avoid the inaccuracies and difficulties encountered in the utilization of the von Karman equations, a modified form of the dimensionless velocity distribution equation of van Driest (Heat Transfer and Mechanics Institute, Paper No. XII, U. of Calif., 1955) has been employed to express the velocity and velocity gradient in the region adjacent to the pipe wall. A new empirically developed velocity distribution equation, based on existing experimental data, has been developed and presented in the course of this study to express the velocity and velocity gradient over the remaining region of flow within the pipe. This equation is of such a nature that when it is used in conjunction with the van Driest equation, the velocity and velocity gradient become continuous functions over the entire region of flow. Utilizing these equations no assumptions are necessary as to the relative magnitude of the molecular and eddy diffusivities of momentum and heat or as to the existence of laminar and transition regions of flow within the pipe.

The fundamental concept of all momentum-heat transfer analogy techniques is predicated upon the assumption that a functional relationship exists between the eddy diffusivities of momentum and heat within the system. In this investigation this relationship is expressed by the parameter σ, defined as the ratio of the eddy diffusivities, and has been included as an independent parameter in the mathematical development. The results of several analytical and experimental investigations have succeeded in establishing limiting maximum and minimum values for σ but this parameter remains far from being completely understood. A mean value of unity has been employed for σ in the numerical computations of this study but the results can be easily re-evaluated for a mean value other than unity.

Based on the above mentioned velocity distribution equations and the parameter σ, the present investigation presents an analytical solution of the momentum and energy equations for a turbulently flowing fluid in a round pipe. Two cases have been considered in the solution of the energy equation. One case is that of a constant heat flux at the pipe wall, which is tantamount to a linear temperature distribution at the pipe wall, and the other is for the case of a constant temperature along the pipe wall. The character of the equations developed is such that the temperature distribution across the pipe can be found directly by numerical integration for the constant heat flux case and by iterative techniques for the constant wall temperature case. The heat transfer coefficient for the system can then be computed directly by employing this temperature distribution.

There is also presented in this study a discussion of some of the physical phenomena which can occur in practical heat transfer applications which are not included in the analytical solution of the momentum and energy equations. The following conclusions have been drawn concerning these phenomena. 1. The theory predicts heat transfer coefficients which are too high for liquid metals at low Reynolds number values due to axial conduction. 2. The heat transfer coefficient of a system which consists of rough pipe may be as much as fifteen per cent higher than that of the same system with smooth pipe. 3. For systems employing a liquid heat transfer fluid, phenomena such as gas entrainment or a fluid which does not "wet" the pipe wall may exhibit heat transfer coefficients considerably lower than would be predicted by the theory.

All except the first of these phenomena are discussed only qualitatively due to a lack of sufficient experimental data to draw definite quantitative results.

Values of the heat transfer coefficient in the form of Nusselt number have been computed for both the case of constant heat flux at the pipe wall and constant temperature at the pipe wall for values of Prandtl number ranging from 0.01 to 100 and values of Reynolds number from 5,000 to 10,000,000. Values of Nusselt number for Peclet numbers less than 150 have been corrected for axial conduction by employing a semi-empirical correlation postulated by Trefethen (Transactions of the American Society of Mechanical Engineers, 78, 1207-1212, 1956).

The values calculated in this investigation have been compared with the existing experimental data and with the values predicted by Rannie (Heat Transfer in Turbulent Shear Flow, Ph.D. Thesis, California Institute of Technology, 1951) for fluids with Prandtl numbers equal to or greater than one and with the predictions of Martinelli (Transactions of the American Society of Mechanical Engineers, 69, 947-959, 1947) and Seban and Shimazaki (Transactions of the American Society of Mechanical Engineers, 73, 803-809, 1951) for liquid metals.

The heat transfer coefficients predicted in this investigation compare favorably with experimental data over wide ranges of Prandtl number and Reynolds number. The results also indicate that fluids with Prandtl number less than unity exhibit substantially different heat transfer coefficients depending upon the wall temperature distribution.

CHAPTER I

INTRODUCTION

Empirical correlations for the prediction of heat transfer coefficients for ordinary fluids in turbulent motion in conduit have existed for many decades. With the advent of liquid metals and fused salts as heat transfer fluids, however, it was discovered that the existing empirical correlations were inadequate for predicting heat transfer coefficients for fluids with Prandtl numbers considerably different from unity. Many theoretical and experimental investigations have been performed in the past decade in an effort to solve this problem.

One of the most promising methods among the theoretical techniques has been the prediction of heat transfer coefficients by analogy with the transfer of momentum. The development and use of these analogy methods, together with various other approaches to the calculation of heat transfer coefficients, have been reviewed by Summerfield (1), Jakob (2) (3), and Knudsen and Katz (4). (Additional references not contained in these reviews or cited in this work are contained in the bibliography.) It was the purpose of this investigation to examine further the prediction of heat transfer coefficients of turbulently flowing fluids in round pipe by momentum-heat transfer analogy methods.

Although momentum-heat transfer analogy methods are theoretical in nature, they necessarily employ two quantities which to date can be obtained only empirically. These are the radial temperature distribution within the pipe and the functional relationship between the eddy

diffusivities of momentum and heat. Von Karman (5) proposed the use of Nikuradse's (6) velocity data for smooth pipe in the form of a dimensionless velocity distribution. With this distribution, along with certain other assumptions as to the behavior of the fluid in various regions within the pipe, he was able to calculate a temperature distribution and hence the heat transfer coefficient for the fluid. Since that time nearly all analogy methods have been based on this "universal" velocity distribution. There are, however, several limitations to this distribution; they are discussed in Chapter II. The method of handling the limitations of the Von Karman equations and the variation of the use of simplifying assumptions comprise the differences in the vast majority of momentum-heat transfer analogy models postulated. Among the outstanding investigations in which the Von Karman temperature distribution was not used are those of Deissler and Eian (7), Deissler (8), Rannie (9), Reichardt (10) (11), and van Driest (12).

As stated above, analogy methods assume a functional relationship exists between the eddy diffusivities of momentum and heat, ϵ_M and ϵ_H, in order to determine the temperature distribution and hence the heat transfer coefficient. This relationship is defined as:

$$\sigma = \frac{\epsilon_H}{\epsilon_M} \qquad \text{(I-1)}$$

Many theoretical and experimental investigations have been performed in an effort to determine the numerical value of σ for various flow conditions. Although these investigations have succeeded in establishing limits for σ, this function remains considerably in question. The

function σ has been assumed by most investigators to have a mean value equal to unity. In this investigation σ has been included as a parameter in all mathematical derivations, although for final numerical computations a value equal to unity has been utilized. The results may easily be re-evaluated for a mean value of σ different from unity. The parameter σ is discussed more fully in Chapter V.

Investigations involving fluids with Prandtl numbers of order of magnitude one or greater have led to the conclusion that the axial temperature distribution along the wall of the conduit has little effect on the heat transfer characteristics of the system. This is not the case, however, for fluids with low Prandtl numbers, such as liquid metals. The majority of the momentum-heat transfer analogy investigations have been done for the case of constant heat flux which renders a linear temperature distribution along the wall of the conduit. Seban and Shimazaki (13) and Hefner (14) have investigated the case of constant temperature at the wall of a round pipe and Sleicher (15), using a mathematical approach proposed by Tribus and Klein (16), has investigated the case of an arbitrary temperature distribution at the pipe wall. All of these investigations illustrate the necessity of considering the wall temperature distribution for fluids with low Prandtl numbers.

In this investigation a mathematical model has been postulated for the prediction of heat transfer coefficients of fluids in fully developed turbulent motion in round pipe. An empirical equation, expressed in dimensionless parameters, has been developed for the radial velocity distribution required by analogy models. This equation is presented in Chapter II along with a general discussion of this type of equation.

Based on the above mentioned velocity distribution equation, the necessary equations for the calculation of the temperature distribution and heat transfer coefficient in the form of the Nusselt number are developed in Chapter III for the case of a constant heat flux at the pipe wall and in Chapter IV for the case of constant temperature at the pipe wall.

Discussion of the parameters affecting the computation of heat transfer coefficients by analogy methods is presented in Chapter V. There is also presented in Chapter V a comparison of the heat transfer coefficients computed in this investigation with existing experimental data and with the theoretical values computed by Martinelli (17) and Franklet (18) for the case of constant heat flux, and those computed by Seban and Shimazaki (13) and Hefner (14) for the case of constant wall temperature.

CHAPTER II

VELOCITY DISTRIBUTION AND EDDY DIFFUSIVITY OF MOMENTUM

For a fluid flowing turbulently within a cylindrical tube, sufficiently far removed from the entrance to insure the absence of end effects, the Reynolds momentum equations reduce to:

$$\frac{g_c}{\rho}\frac{\partial \bar{P}}{\partial x} = \frac{1}{r}\frac{\partial}{\partial r}\left(r\nu\frac{\partial \bar{u}}{\partial r}\right) - \frac{1}{r}\frac{\partial}{\partial r}\left(r\,\overline{u'r'}\right) \qquad \text{(II-1)}$$

The system satisfying this equation is subject to the following restrictions:

a. Steady state conditions exist.

b. Fluid is incompressible.

c. Mean velocity of fluid is in the x-direction, the x-axis coinciding with the center line of the pipe.

d. System is symmetrical about the x-axis.

e. Fluid properties are independent of temperature.

f. Axial diffusion is negligible with respect to the bulk transport of momentum in the x-direction.

If the mean value $\overline{u'v'}$ is defined to be $-\epsilon_M(\partial\bar{u}/\partial r)$, Equation (II-1) becomes:

$$\frac{g_c}{\rho}\frac{\partial \bar{P}}{\partial x} = \frac{1}{r}\frac{\partial}{\partial r}\left(r\nu\frac{\partial \bar{u}}{\partial r}\right) + \frac{1}{r}\frac{\partial}{\partial r}\left(r\,\epsilon_M\frac{\partial \bar{u}}{\partial r}\right) \qquad \text{(II-2)}$$

Based on the postulates listed above, the partial derivatives in Equation (II-2) can be replaced by total derivatives, and hence the equation can be rearranged and integrated once with respect to r to yield:

$$\frac{g_c r}{2\rho} \frac{d\bar{P}}{dx} = - (\nu + \epsilon_M) \frac{d\bar{u}}{dr} \qquad \text{(II-3)}$$

A force balance on a differential annulus of fluid of radius r becomes:

$$\frac{1}{\rho} \frac{d\bar{P}}{dx} = - \frac{2}{r} \frac{\tau}{\rho} \qquad \text{(II-4)}$$

and

$$\frac{\tau}{r} = \frac{\tau_w}{R} \qquad \text{(II-5)}$$

Equation (II-5) can be written as:

$$\frac{\tau}{\rho} = \frac{\tau_w}{\rho} (1 - y/R) \qquad \text{(II-6)}$$

Substitution of Equation (II-4) into Equation II-3) yields:

$$\frac{g_c \tau}{\rho} = - (\nu + \epsilon_M) \frac{d\bar{u}}{dr} = (\nu + \epsilon_M) \frac{d\bar{u}}{dy} \qquad \text{(II-7)}$$

Then on substitution of Equation (II-6) into Equatien (II-7) and rearranging, there is obtained:

$$\epsilon_M = \frac{g_c \tau_w}{\rho} \frac{(1 - y/R)}{d\bar{u}/dy} - \nu \qquad \text{(II-8)}$$

Equation (II-8) can be solved directly for the eddy diffusivity of momentum provided the velocity gradient is known as a function of position, it being previously assumed that the molecular viscosity is constant. To date there have been no successful methods evolved for the theoretical prediction of the velocity distribution or velocity gradient for turbulently flowing fluids in pipes. Many experimental investigations have, therefore, been performed in an effort to express empirically the velocity of a fluid as a function of the many parameters which affect the velocity.

The most notable of the empirical velocity distribution equations was developed by von Karman (5) and was based on the data obtained by Nikuradse (6). This velocity distribution is expressed in terms of dimensionless parameters in order to make it "universally" applicable, and can be written as:

$$u^+ = y^+ \qquad 0 \leq y^+ \leq 5 \qquad \text{(II-9)}$$

$$u^+ = -3.05 + 5.0 \ln y^+ \qquad 5 \leq y^+ \leq 26 \qquad \text{(II-10)}$$

$$u^+ = 5.0 + 2.5 \ln y^+ \qquad y^+ \geq 26 \qquad \text{(II-11)}$$

where $u^+ = \bar{u}/u^*$

$$y^+ = u^* y/\nu$$

$$u^* = \sqrt{g_c \tau_w/\rho}$$

The von Karman velocity distribution is of sufficient accuracy to make it quite useful for many applications. It was pointed out in Chapter I that the majority of momentum-heat transfer analogy models have been developed with the use of this velocity distribution. In spite of its

wide usage, there are many limitations to this distribution which must be taken into consideration in any successful analogy model.

The most obvious of these limitations is the fact that the velocity distribution is expressed by three equations which have oblique points of intersection, thus rendering points of discontinuity in the velocity gradient function. This situation has been alleviated by those models in which the von Karman equations were employed by considering the area of flow as being composed of three distinct regions with the necessary integration of the momentum and energy equations being carried out in stages so as to avoid these points of discontinuity.

A second limitation of the von Karman equations lies in the fact that they are inaccurate in the region very close to the pipe wall. In analogy models developed for prediction of heat transfer coefficients for liquid metals, which exhibit very low Prandtl numbers, this is not a serious limitation and can be disregarded since the region very close to the pipe wall has little effect on the over-all heat transfer characteristics of the system. For fluids with Prandtl numbers of the order of one or greater, however, the region adjacent to the wall contributes a major portion to the over-all resistance to heat flow.

Several investigators have proposed empirical velocity distribution equations for the region adjacent to the pipe wall where the von Karman equations become inaccurate. The most outstanding of these are the equations of van Driest (12) and Deissler (19). Both of these equations appear to give reasonably accurate values for the velocity gradient very close to a wall. The only apparent preference of one of these equations over the other is that the van Driest equation expresses the

velocity gradient as an explicit function of position whereas the Deissler equation is an implicit function. Franklet (18) compared the Nusselt numbers he obtained from his analogy model using the von Karman equations with those he obtained by using the van Driest equation and found the latter gave more accurate results for fluids with Prandtl numbers of order one or greater.

A third limitation of the von Karman equation is that the velocity gradient does not approach zero at the center of the pipe. This is inconsistent with the postulated system. Therefore, when Equation (II-8) is solved for the eddy diffusivity of momentum using the von Karman equations, ϵ_M goes through zero and approaches $-\nu$ at the center of the pipe. This, of course, is contrary to the physical situation and unless this situation is rectified, serious errors are introduced into the analogy model.

Most investigators, when employing the von Karman equations, have assumed the numerical value of the molecular viscosity negligible compared to the eddy diffusivity of momentum in the region of fully developed turbulence. This assumption is quite justified over a large portion of the flow regime where ϵ_M is 100 to 1000 times greater than ν. The erroneous negative values of ϵ_M are avoided in Equation (II-8) when this assumption is made, but again the solution of Equation (II-8) near the center of the pipe, assuming ν is negligible, is in contrast to the assumed situation. That is, as the center of the pipe is approached, ϵ_M approaches zero and hence approaches and even becomes less than the numerical value of ν.

Von Karman chose as the parameters of his velocity distribution equation the quantities u^+ and y^+. This appears to be a justifiable

choice for if the data for a large number of fluids over wide ranges of Reynolds are plotted on a single graph as u^+ vs. $\ell n\ y^+$, the points can be fitted quite closely by a single straight line for y^+ values greater than about thirty. The equation of this line becomes Equation (II-11).

If the points on such a graph are examined more critically, however, it can be seen that they do not deviate from the best straight line in a random manner. Rather, the points for a particular bulk Reynolds number begin to curve away from the line and approach a constant value of u^+ as the maximum y^+ value for that Reynolds number is approached. This situation is demonstrated in Fig. 1 where a curve has been faired in for the points of an individual bulk Reynolds number. The reason for this deviation is explained by the fact that this maximum y^+ value represents the center line of the pipe where the velocity gradient is zero. It can be seen that the center line value of the parameter y^+ is a function of the properties of the fluid and the Reynolds number. It, therefore, becomes difficult to develop an equation for the velocity distribution in which it is required that the gradient go to zero at the pipe center when the parameter y^+ is employed.

An alternate pair of dimensionless parameters which can be applied to velocity data are u^+ and y/R. The parameter y/R has the advantage that the pipe wall and center line are easily distinguishable as 0 and 1, respectively. When the data of various fluids at varying Reynolds numbers are plotted as u^+ vs. $\ell n(y/R)$, they do not form a single curve, however, as was the case for the parameters u^+ and y^+. Fig. 2 is a typical plot of this type employing some of Nikuradse's data.

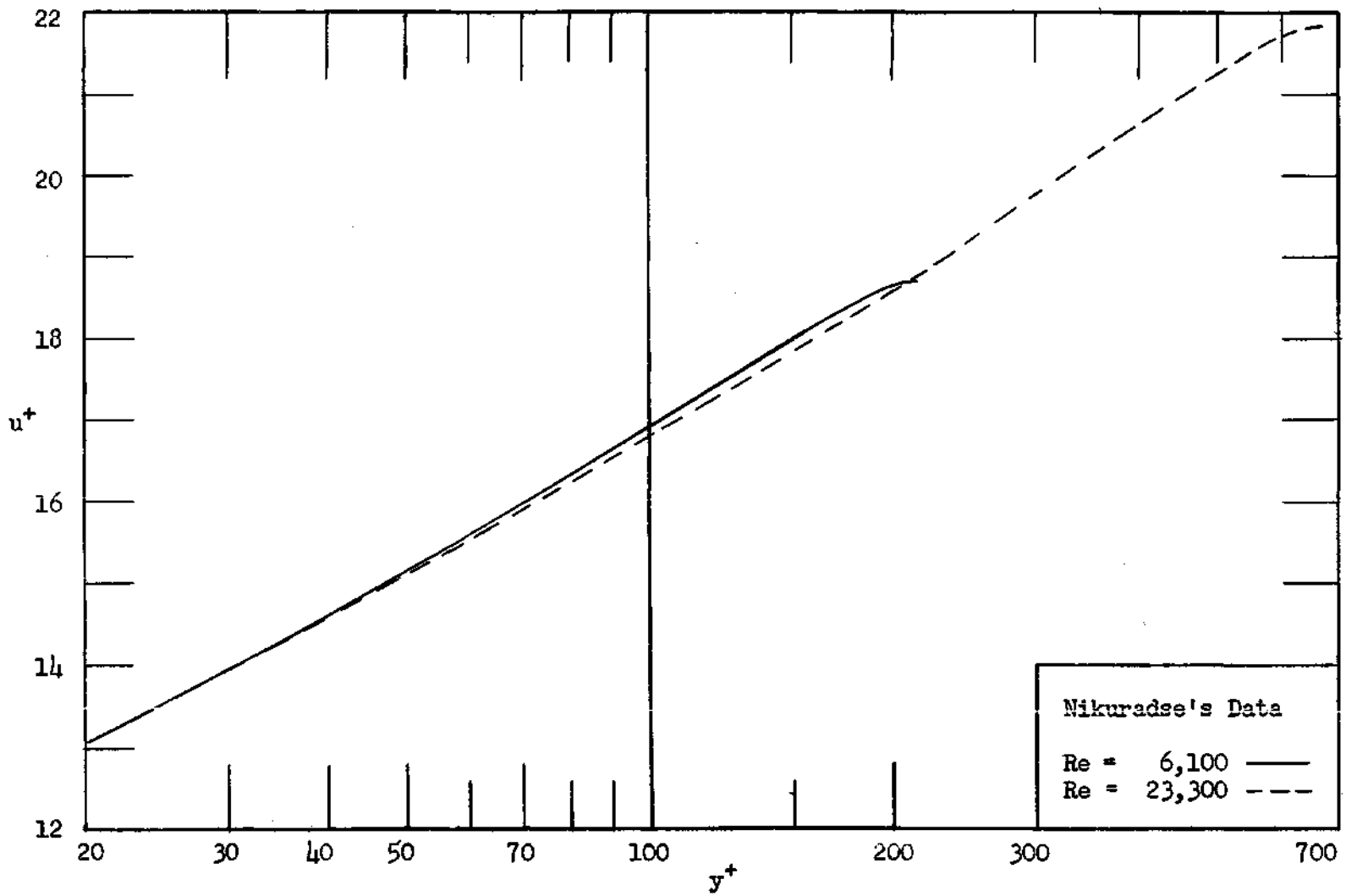

Figure 1. Radial Velocity Distribution Profiles

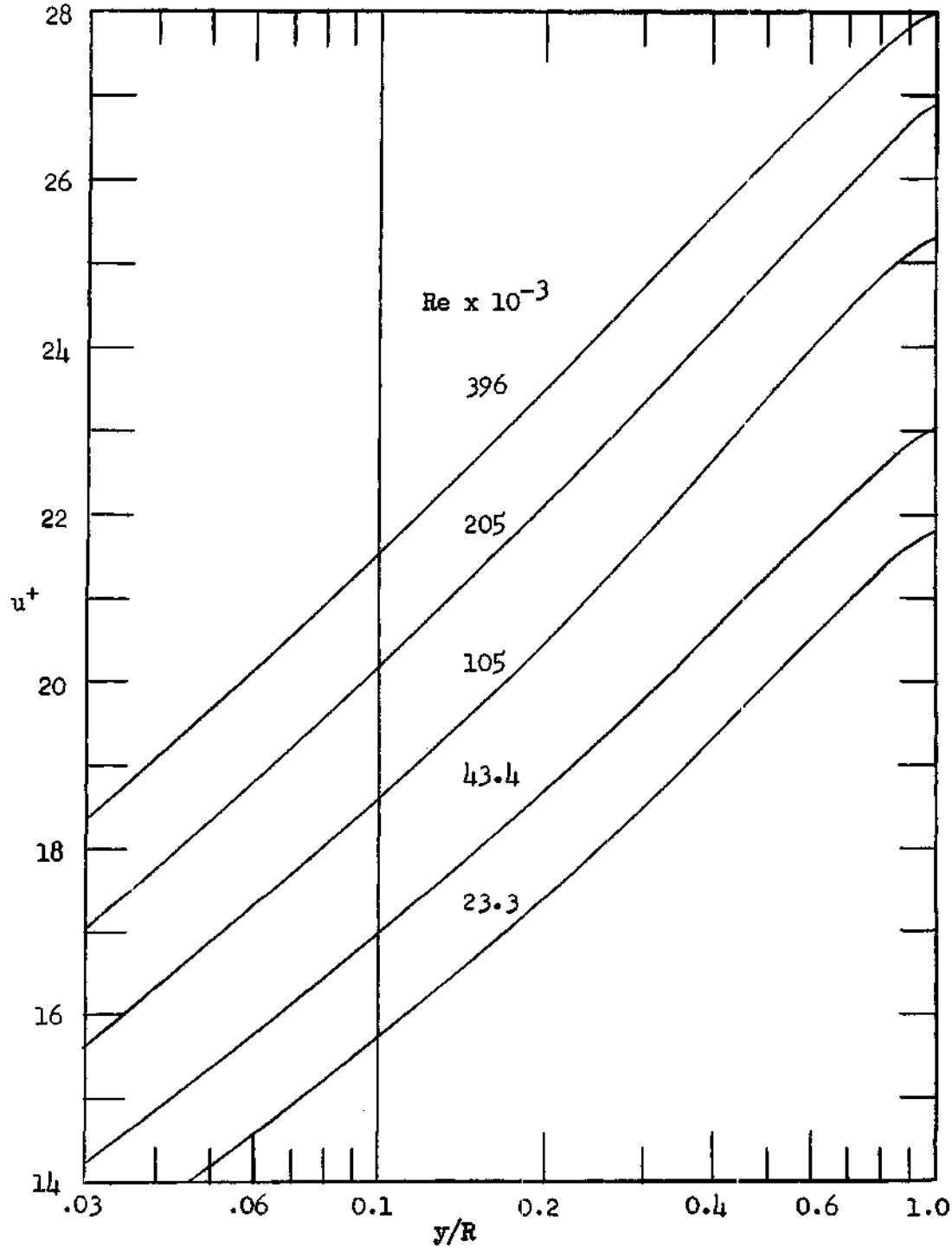

Figure 2. Fluid Velocity as a Function of Radial Position

When velocity data are fitted by curves for the parameters u^+ and y/R, it has been found that the center line values of u^+, at $y/R = 1$, can be expressed empirically as a function of the bulk Reynolds number or the parameter $Re^* \equiv Du^*/\nu$, which one might refer to as the "friction velocity" Reynolds number.

The family of curves formed by these parameters are not parallel since they must all converge to $u^+ = 0$ at $y/R = 0$. Hence, the velocity gradient must be a function of some third parameter and, again, it has been found that either the bulk Reynolds number of Re^* can be used for this third parameter.

For a velocity distribution equation to be useful in momentum-heat transfer analogy techniques, it must accurately express the velocity gradient as well as the velocity at a point. To develop such an equation empirically, then, requires accurate velocity gradient data. Velocity gradients are difficult to measure directly and hence are usually obtained from velocity distribution data by numerical techniques. The most common method of obtaining derivatives from discrete data points is the use of quadrature formulas based on Lagrangian polynomials. The accuracy of such quadrature formulas is dependent upon the ability to express the unknown function by a polynomial. A common misnomer concerning this type of quadrature formula is that the error decreases as the order of the quadrature formula is increased. It is true that the error term is directly proportional to an ever increasing power of the interval between data points, which, if this interval is small, produces a progressively smaller number. However, the error term is also directly proportional to a higher and higher order derivative of the function at

some point in the region, which, if the function is of such nature that it cannot be accurately approximated by a polynomial, may increase faster than the elevated power of the interval decreases. The reader is referred to such texts as Willers (20), Hildebrand (21), or Kopal (22) for a more thorough discussion of this subject.

It has been demonstrated by several investigators that turbulent velocity distribution data are not well suited to polynomial fits. This should not be construed to mean that velocity gradients obtained by Lagrangian polynomial quadrature formulas are not valid. This reasoning is mentioned to illustrate the importance of applying additional quadrature formulas obtained from other interpolating functions in the critical regions very near the wall and center line of the pipe to ensure the highest possible accuracy of the velocity gradient in these regions.

Quadrature formulas based on various interpolating functions have been applied to the data of Nikuradse (6), Pannel (23), Isakoff and Drew (24), and Weisberg (25). The mean values of the gradients obtained for certain of Nikuradse's data are compared in Table 1 to those obtained graphically by Nikuradse and those obtained from the von Karman equations.

In the course of processing the above mentioned velocity data and velocity gradients obtained therefrom, all attempts at fitting a single function which would fit both the velocity and velocity gradient data over the entire region of flow were too cumbersome and lengthy to be of practical use. Also, since the van Driest equation fit all the available data quite well in the region adjacent to the pipe wall, it was decided to use that equation in the proximity of the wall and develop a new equation to fit the remaining region of flow.

Table 1. Velocity Gradients Obtained from Data of Nikuradse

Nikuradse's graphical determination: $(\frac{d\bar{u}}{dy})_N$

This study: $(\frac{d\bar{u}}{dy})_H$

Von Karman equations: $(\frac{d\bar{u}}{dy})_{vk}$

Re = 43,400

$\bar{u}$ = 258.2 cm/sec

u* = 13.46 cm/sec

v = 0.0119 cm^2/sec

R = 1.0 cm

y	$\bar{u}$	$(\frac{d\bar{u}}{dy})_N$	$(\frac{d\bar{u}}{dy})_H$	$(\frac{d\bar{u}}{dy})_{vk}$
0.02	183.0	1348	2366	2677
0.04	203.0	693	872	935
0.07	220.0	411	451	534
0.10	230.0	302	345	374
0.15	242.5	220	228	249
0.20	252.0	181	186	187
0.30	267.0	129	128	125
0.40	278.5	99	95	93
0.50	287.0	81	77	75
0.60	294.5	68	59	62
0.70	300.0	55	51	53
0.80	304.5	44	45.8	47
0.90	308.7	30	40.2	42
0.96	309.6	18.5	33.8	38.9
0.98	310.0	13.0	27.5	38.2
1.00	310.5		0	37.4

With the use of an IBM 650 at the Rich Electronic Computer Center at the Georgia Institute of Technology, least squares techniques were applied to various functions in an effort to fit the data to an empirical function. The following equation was considered to be the best of the ones developed.

$$u^+ = 4.0986 + 2.778 \ln Re^* - \frac{1}{\ln Re - 7} +$$

$$(2.7660 + 0.00125 \ln Re^*) [\ln(y/R) - 0.10 (y/R)^{10}] \quad \text{(II-12)}$$

where $70/Re^* \leq y/R \leq 1$.

In terms of the velocity gradient, Equation (II-12) becomes:

$$\frac{du^+}{d(y/R)} = (2.7660 + 0.00125 \ln Re^*) [\frac{1}{y/R} - (y/R)^9] \quad \text{(II-13)}$$

where $70/Re^* \leq y/R \leq 1$.

The van Driest equation, for the region adjacent to the pipe wall, can be written as:

$$\frac{du^+}{d(y\ R)} = \frac{Re^*(1-y/R)}{1 + \{1+0.16(1-y/R)(Re^*/y/R)^2\ [1-\exp(-\frac{Re^*y/R}{54})]^2\}^{1/2}} \quad \text{(II-14)}$$

where $0 \leq y/R \leq 70/Re^*$.

The van Driest equation cannot be integrated in closed form, hence, the velocity at a point must be obtained by numerical integration.

Equations (II-12) and II-13) merge smoothly with the van Driest equation for both the velocity and velocity gradient. Table 2 gives the values of these quantities computed for several values of Re* and y/R by

Table 2. Velocities and Velocity Gradients Obtained from van Driest Equation (vD), This Study (H) and von Karman Equations (vk)

Re*	y/R = 56/Re*			y/R = 70/Re*			y/R = 140/Re*		
	u^+_{vD}	u^+_H	u^+_{vk}	u^+_{vD}	u^+_H	u^+_{vk}	u^+_{vD}	u^+_H	u^+_{vk}
283	14.43	14.51	13.05	15.10	15.12	13.68	16.72	17.02	17.57
2,262	14.92	15.08	13.05	15.67	15.70	13.68	17.66	17.62	17.57
28,340	14.98	16.15	13.05	15.75	15.75	13.68	17.76	17.67	17.57
1,110,000	14.99	15.18	13.05	15.75	15.76	13.68	17.80	17.78	17.57
	$\frac{du^+}{d(y/R)_{vD}}$	$\frac{du^+}{d(y/R)_H}$	$\frac{du^+}{d(y/R)_{vk}}$	$\frac{du^+}{d(y/R)_{vD}}$	$\frac{du^+}{d(y/R)_H}$	$\frac{du^+}{d(y/R)_{vk}}$	$\frac{du^+}{d(y/R)_{vD}}$	$\frac{du^+}{d(y/R)_H}$	$\frac{du^+}{d(y/R)_{vk}}$
283	16.25	15.81	25.25	11.42	11.38	10.12	3.79	4.01	5.06
2,262	144.1	131.8	201.6	104.1	100.3	809	49.73	56.27	40.45
28,340	1828	1625	2525	1325	1304	1012	68.5	89.3	50.6
1,110,000	7145	6216	9881	5181	4920	3968	2795	3135	1984

use of Equations (II-12) and (II-13), the van Driest equation and the van Karman equations. From this table it can be seen that the equations of this study yield essentially the same values for both the velocity and velocity gradients as the van Driest equation over the region 56/Re* to 140/Re*. The transition from one equation can, hence, be taken anywhere within this range with high accuracy. The value 70/Re* has been found to be the midpoint of the region coincidence and therefore has been selected as the limiting value of y/R for the two equations. It can be seen that the values obtained from the von Karman equations differ considerably from either of the other two equations.

With the utilization of Equation (II-13) and (II-14) the eddy diffusivity can be computed as a function of position within the pipe from Equation (II-8). It is interesting to note that in employing this procedure no assumptions are necessary as to the relative magnitudes of the quantities ν and ϵ_M. Fig. 3 compares the eddy diffusivities of momentum computed by Equations (II-13) and (II-14) with the experimental data of Sage, et al. (26), taken between parallel plates, and with these values computed by the von Karman equations.

It can be seen that the numerical value of ϵ_M as computed from Equation (II-8), employing Equation (II-13), does not approach zero at the center of the pipe. The question of what the numerical value of ϵ_M at the pipe center should be is one that has been argued in the literature for some time. Many investigators feel that ϵ_M should go to zero at the center line, some feel it should approach ν, and still others feel it will have some other positive value. The question is not one that can

be solved from a purely mathematical standpoint for at the center of the pipe $d\bar{u}/dy$ is zero, and hence Equation (II-8) becomes indeterminant. If Equation (II-6) is substituted into Equation (II-7), the result is:

$$\frac{g_c \tau_w}{\rho} (1 - y/R) = (\nu + \epsilon_M) \frac{d\bar{u}}{dy} \qquad \text{(II-15)}$$

Now, at the center line $(1 - y/R)$ and $d\bar{u}/dy$ both equal zero and hence Equation (II-15) becomes:

$$\frac{g_c \tau_w}{\rho} (0) = (\nu + \epsilon_M) (0) \qquad \text{(II-16)}$$

and, thus, it can be seen that from a mathematical standpoint, ϵ_M can take on any finite value and Equation (II-16) will still be satisfied.

An intuitive argument can be applied to the situation from Equation (II-1), however. The eddy diffusivity of momentum is actually a function of the product of the fluctuating components in the x and y direction, $\overline{u'v'}$. Now at the center of the pipe the net transport of momentum is zero. This does not imply, however, that the fluctuating velocity components are zero. Since the eddy diffusivity of momentum is in essence a measure of these fluctuating components, it is reasonable to assume that ϵ_M should be greater than zero at the pipe center.

Efforts have been made by several investigators to determine experimentally the numerical value of ϵ_M, but again the conclusions are varied. It is extremely difficult to measure velocities with high precision near the center of a pipe because of the fluctuations due to turbulence. And, as it was previously pointed out, since the velocity

gradient can only be obtained from velocity data, these values are difficult to obtain precisely. In this critical region very near the pipe center, $(1 - y/R)$ and $d\bar{u}/dy$ are very small; therefore, a small error in either quantity can cause large errors in the evaluation of ϵ_M. Consequently, different experimenters have arrived at quite conflicting results. The data of Sage, et al. (26), given in Fig. 3 when extrapolated to the center line would appear to give a value of ϵ_M considerably greater than zero. This is not universally the case with the data of all investigators, however.

Based on Equations (II-12) and (II-14), equations are developed in Chapters III and IV for the prediction of heat transfer coefficients by analogy to momentum transfer.

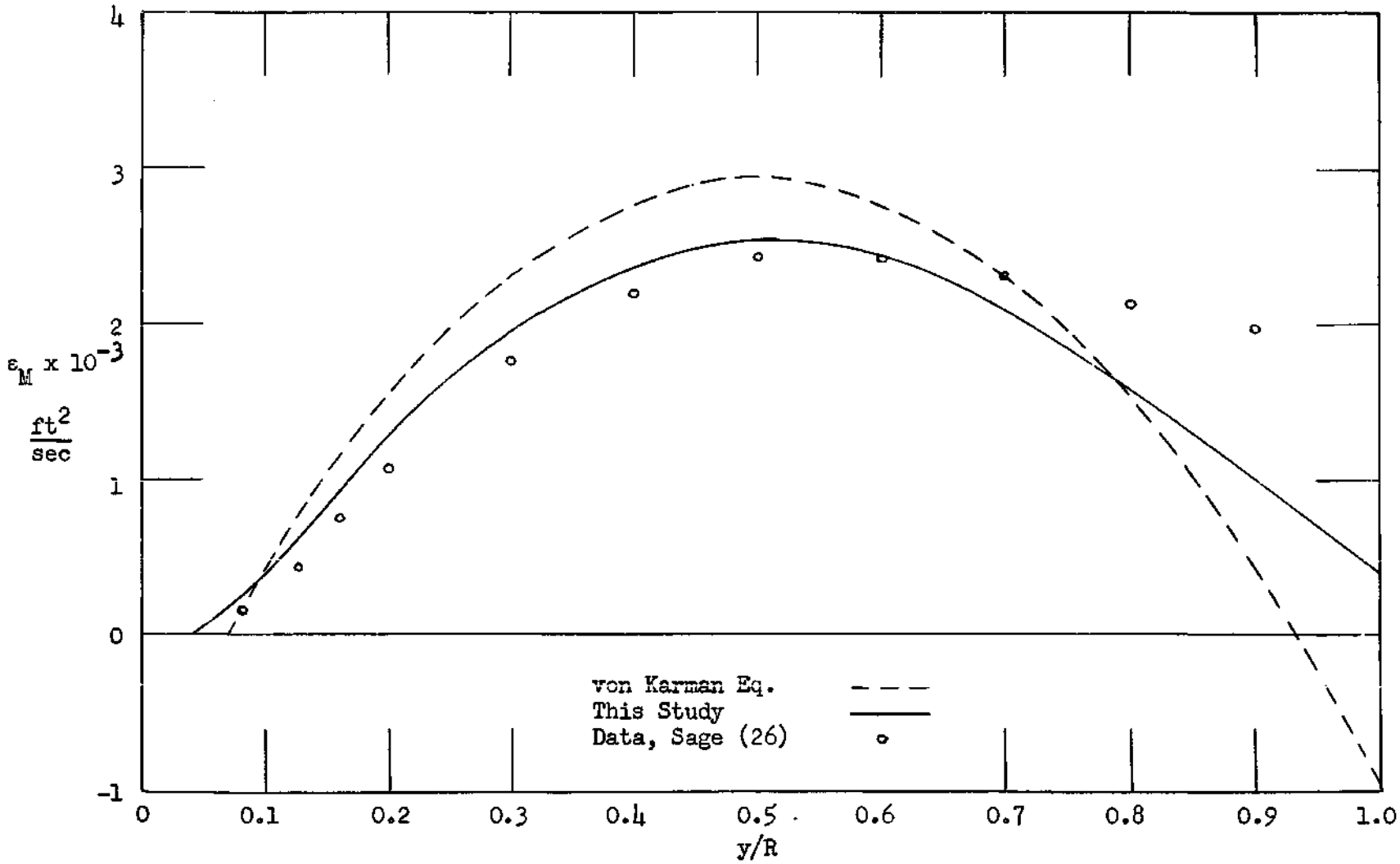

Figure 3. Eddy Diffusivity of Momentum as a Function of Radial Position

CHAPTER III

TEMPERATURE DISTRIBUTION AND HEAT TRANSFER COEFFICIENTS FOR CONSTANT HEAT FLUX

The energy equation for the system described in Chapter II for the turbulent flow of a fluid in a cylindrical tube reduces to:

$$\bar{u}\frac{\partial \bar{t}}{\partial x} = \frac{1}{d}\frac{\partial}{\partial r}\left(r\,\alpha\,\frac{\partial \bar{t}}{\partial r}\right) - \frac{1}{r}\frac{\partial}{\partial r}\left(r\,\overline{v't'}\right) \qquad \text{(III-1)}$$

The system satisfying this equation is contingent on the following additional restrictions:

(g) Dissipative effects are negligible.

(h) Axial transfer of heat is negligible with respect to the bulk transfer in the radial direction.

An energy balance on a differential annulus of fluid of radius r and length Δx yields:

$$\bar{u}\frac{\partial \bar{t}}{\partial x} = \frac{1}{2\pi r \rho C_p \Delta x}\frac{\partial q}{\partial r} \qquad \text{(III-2)}$$

Defining $\overline{v't'}$ as $-\epsilon_H(\partial \bar{t}/\partial r)$ and substituting Equation (III-2) into Equation (III-1), there is obtained:

$$\frac{1}{2\pi r \rho C_p \Delta x}\frac{\partial q}{\partial x} = \frac{1}{r}\frac{\partial}{\partial r}\left(r\,\alpha\,\frac{\partial \bar{t}}{\partial r}\right) + \frac{1}{r}\left(r\,\epsilon_H\,\frac{\partial \bar{t}}{\partial r}\right) \qquad \text{(III-3)}$$

Based on the given postulates that axial transfer of heat is negligible compared to the radial transfer, the partial derivatives with respect to r can be replaced by total derivaties in Equations (III-2) and (III-3). Hence, Equation (III-3) can be integrated once with respect to r, since $\partial\bar{t}/\partial x$ is constant for constant heat flux, to yield:

$$\frac{q}{A_r \rho C_p} = (\alpha + \epsilon_H) \frac{d\bar{t}}{dr} = (\alpha + \epsilon_H) \frac{d\theta}{dy} \qquad \text{(III-4)}$$

where $\theta = t_w - \bar{t}$

$A_r = 2\pi r \Delta x$.

Equation (III-2) can also be integrated with respect to radius to become:

$$q_w = u_m (\pi R^2 \Delta x) \rho C_p \frac{\partial t}{\partial x} \qquad \text{(III-5)}$$

Substitution of Equation (III-5) into Equation (III-2) yields:

$$\frac{dq}{dr} = q_w \frac{\bar{u}}{u_m} \frac{2r}{R^2} \qquad \text{(III-6)}$$

Now, if it is assumed for purposes of Equation (III-6) that $\bar{u} = u_m$ for all $\bar{u}$, that equation can be integrated to give:

$$q = q_w \frac{r^2}{R^2} \qquad \text{(III-7)}$$

or

$$\frac{q}{A_r} = \frac{q_w}{A_w} \frac{r}{R} = \frac{q_w}{A_w} \left(1 - \frac{y}{R}\right) \qquad \text{(III-8)}$$

The assumption made that $\bar{u} = u_m$ for all $\bar{u}$ in Equation (III-6) seems unjustified. The resulting equation, however, which states that the heat flux is a linear function of the radial position, is substantiated by experimental measurements.

Substitution of Equation (III-8) into Equation (III-4) and rearrangement yields:

$$d\theta = \frac{q_w}{A_w \rho C_p} \frac{(1 - y/R)}{(\alpha + \epsilon_H)} dy \qquad \text{(III-9)}$$

which can be written as:

$$d\theta = \frac{q_w R}{A_w \rho C_p \sigma \bar{v}} \frac{1 - y/R}{(\epsilon_H/\sigma\nu) + (\alpha/\sigma\nu)} d(y/R) \qquad \text{(III-10)}$$

Defining the ratio of the eddy diffusivities of heat and momentum by the following equation:

$$\sigma \equiv \frac{\epsilon_H}{\epsilon_m} \qquad \text{(III-11)}$$

Equation (III-10) can be expressed as:

$$d\theta = \frac{q_w R}{A_w \rho C_p \sigma \bar{v}} \frac{(1 - y/R)}{(\epsilon_M/\nu) + (1/\sigma P_r)} d(y/R) \qquad \text{(III-12)}$$

Integration of Equation (III-12) yields:

$$\theta = \frac{q_w R}{A_w \rho C_p \sigma \bar{v}} f(w) \qquad \text{(III-13)}$$

where for simplicity of notation:

$$f(w) \equiv \int_{o}^{w} \frac{(1 - y/R)}{(\epsilon_M/\nu) + (1/\sigma P_r)} \, d(y/R) \qquad \text{(III-14)}$$

for $0 \leq w \leq 1$.

The heat transfer coefficient for the system can be defined as:

$$q_w = hA_w(t_w - t_m) = hA_w\theta_m \qquad \text{(III-15)}$$

Therefore, the Nusselt number can be expressed as:

$$Nu = \frac{hD}{k} = \frac{q_w D}{A_w k \theta_m} = \frac{q_w PrRe\lambda}{\rho C_p A_w u^* \theta_m} \qquad \text{(III-16)}$$

where

$$\theta_m = \frac{\int_o^R \theta \bar{u} r dr}{\int_o^R \bar{u} r dr} = \frac{2}{u_m R^2} \int_o^R \theta \bar{u} r dr \qquad \text{(III-17)}$$

Equation (III-17) can be expressed as:

$$\theta_m = \frac{2u^*}{u_m} \int_o^R \theta u^+ (1 - y/R) \, d \, (y/R) \qquad \text{(III-18)}$$

From the definition of the friction factor it follows that:

$$u^* = u_m \sqrt{f/8} = u_m \lambda \qquad \text{(III-19)}$$

Hence, Equation (III-18) becomes:

$$\theta_m = 2\lambda \int_0^R \theta u^*(1 - y/R)\, d\,(y/R) \qquad \text{(III-20)}$$

Substitution of Equation (III-13) into Equation (III-20) yields:

$$\theta_m = \frac{2q_w R\lambda}{A_w \rho C_p \sigma \nu} \; F(R) \qquad \text{(III-21)}$$

where, for simplicity of notation:

$$F(R) \equiv \int_0^R f(w)u^+ \,(1 - w)dw \qquad \text{(III-22)}$$

Therefore, substitution of Equation (III-22) into Equation (III-16) yields an expression for the heat transfer coefficient of the system which can be written as:

$$Nu = \frac{\sigma PrRe}{Re^*F(R)} \qquad \text{(III-23)}$$

In order to obtain numerical values for the temperature distribution from Equation (III-13) and for the heat transfer coefficient from Equation (III-23), it becomes necessary to employ the equations developed in Chapter II. Thus, Equation (II-8) can be expressed as:

$$\epsilon_M = \frac{u^*R(1 - y/R)}{du^+/d(y/R)} - \nu \qquad \text{(III-24)}$$

or

$$\frac{\epsilon_M}{\nu} = \frac{Re^*}{2} \frac{1 - y/R}{du^+/d(y/R)} - 1 \qquad \text{(III-25)}$$

Substitution of Equation (III-25) into Equation (III-14) yields:

$$f(w) = \int_0^w \frac{(1 - y/R)\, d\,(y/R)}{\frac{Re^*(1 - y/R)}{2\, du^+/d(y/R)} - 1 + \frac{1}{Pr}} \qquad \text{(III-26)}$$

where $0 \leq w \leq 1$.

Introducing Equations (II-12) and (II-14) into Equation (III-26) and considering the two regions to which they apply, the following equations are obtained for the temperature distribution and heat transfer coefficient for a system at constant heat flux.

Region Adjacent to the Wall

$$\frac{du^+}{d(y/R)} = \frac{Re^*(1 - y/R)}{1 + \{1 + 0.16(1 - y/R)(Re^*y/R)^2[1-\exp(-\frac{Re^*y/R}{54})]^2\}^{1/2}} \qquad \text{(III-27)}$$

where $0 \leq y/R \leq 70/Re^*$.

$$f_1(w) = \int_0^w \frac{(1 - y/R)\, d\,(y/R)}{\{1 + 0.16(1 - y/R)(Re^*y/R)^2[1-\exp(-\frac{Re^*y/R}{54})]^2\}^{1/2} + \frac{1}{\sigma Pr}}$$

(III-28)

where $0 \leq w \leq 70/Re^*$.

$$F_1(z) = Re^* \int_0^z f_1(w)(1-w) \int_0^w \frac{(1 - y/R)\, d\,(y/R)}{1+\{1+0.16(1-y/R)(Re^*y/R)^2[1-\exp(-\frac{Re^*y/R}{54})]^2\}^{1/2}} dw$$

(III-29)

where $0 \leq z \leq 70/Re^*$.

$$\theta_1 = \frac{q_w R}{A_w \rho C_p \sigma v} f_1(w) \qquad \text{(III-30)}$$

Region of Fully Developed Turbulence

$$\frac{du^+}{d(y/R)} = (2.7660 + 0.00125 \ \ell n \ Re^*)\left[\frac{1}{y/R} - (y/R)^9\right] \qquad \text{(III-31)}$$

where $70/Re^* \leq y/R \leq 1$.

$$f_2(w) = \int_{70/Re^*}^{w} \frac{(1 - y/R)\, d\,(y/R)}{\dfrac{Re^*(1 - y/R)\,(y/R)}{(5.532+0.0025\ \ell nRe^*)[1-(y/R)^{10}]} - 1 + \dfrac{1}{Pr}} \qquad \text{(III-32)}$$

where $70/Re^* \leq w \leq 1$.

$$F_2(z) = F_1(70/re^*) + \int_{70/Re^*}^{z} [f_1(w) + f_2(w)]\,(1-2)[4.0986 + 2.778\ \ell nRe^*$$

$$- \frac{1}{\ell n\ Re - 7} + (2.7760 + 0.00125\ \ell nRe^*)\ [\ell nw - 0.10\ w^{10}]]dw \qquad \text{(III-33)}$$

where $70/Re^* \leq z \leq 1$.

$$\theta_2 = \frac{q_w R}{A_w \rho C_p \sigma v}\ [f_1(70/Re^*) + f_2(w)] \qquad \text{(III-34)}$$

$$\theta_2 = \theta_1 + \frac{q_w R}{A_w \rho C_p \sigma v}\ f_2(w) \qquad \text{(III-35)}$$

Substitution of the appropriate temperature and velocity distributions into Equation (III-23) gives the following equation for the heat transfer coefficient of the system:

$$\frac{1}{Nu} = \frac{Re^*}{PrRe}\left\{ Re^* \int_0^{70/Re^*} (1-w) \int_0^w \frac{(1 - y/R)\, d\,(y/R)}{1+\{1+0.016(1-y/R)(Re^*y/R)^2[1-\exp(-\frac{Re^*y/R}{54})]^2\}^{1/2}} \, x \right.$$

$$\int_0^w \frac{(1 - y/R)\, d\,(y/R)}{\{1+0.16(1-y/R)(Re^*y/R)^2[1-\exp(-\frac{Re^*y/R}{54})]^2\}^{1/2} + \frac{1}{\sigma Pr}} +$$

$$\int_{70/Re^*}^1 \left[\int_{70/Re^*}^1 \frac{(1 - y/R)\, d\,(y/R)}{\{1+0.16(1-y/R)(Re^*y/R)^2[1-\exp(-\frac{Re^*y/R}{54})]^2\}^{1/2} + \frac{1}{\sigma Pr}} + \right.$$

$$\left. \int_{70/Re^*}^1 \frac{(1 - y/R)\, d\,(y/R)}{\frac{Re^*\,(1 - y/R)\,(y/R)}{(5.532+0.0025\ \ell nRe)[1-(y/R)^{10}]} - 1 + \frac{1}{\sigma Pr}} \right] (1 - w) \, x$$

$$\left. \{4.0986 + 2.778\ \ell n\ Re^* - \frac{1}{\ell n\ Re - 7} + (2.7760 + 0.00125\ \ell n\ Re^*)\, x \right.$$

$$\left. [\ell n\ w - 0.10\ w^{10}]\}\, dw \right\} \qquad \text{(III-36)}$$

This equation was solved by utilizing an IBM 650 digital computer. The trapezoidal rule was employed for the indicated integrations with thirty intervals taken in the region 0 to 70/Re* and fifty intervals taken in the region 70/Re* to 1. As a check, the number of intervals was increased to fifty and eighty for Pr = 0.02 and Re = 10^6. There was a difference of less than one per cent in the value of the Nusselt number obtained with the smaller increments.

CHAPTER IV

TEMPERATURE DISTRIBUTION AND HEAT TRANSFER COEFFICIENTS FOR CONSTANT WALL TEMPERATURE

The energy equation for the system under consideration, based on the previously listed postulates, can be written as:

$$R^2 u^* {}^2 u^+ \frac{\partial \theta}{\partial x} = \frac{1}{(1-y/R)} \frac{d}{d(y/R)} \left[(1-y/R)(\alpha+\epsilon_H) \frac{d\theta}{d(y/R)} \right] \qquad \text{(IV-1)}$$

Since $\partial\theta/\partial x$ is not a constant for the case of constant temperature at the pipe wall, Equation (IV-1) cannot be integrated with respect to r in its present form. The following lemma is proved in Appendix I, however:

$$\frac{\partial \theta}{\partial x} = \frac{\theta}{\theta_m} \frac{\partial \theta_m}{\partial x} \qquad \text{(IV-2)}$$

Thus, substituting Equation (IV-2) into Equation (IV-1) and rearranging, the integration can be performed, since $\partial\theta_m/\partial x$ is independent of r, to yield:

$$R^2 u^* \frac{\partial \theta_m}{\partial x} \int_o^w \frac{\theta}{\theta_m} u^+ (1 - y/R)\, d\,(y/R) = (1 - w)(\alpha + \epsilon_H) \frac{d\theta}{dw} \qquad \text{(IV-3)}$$

where $1 \leq w \leq 0$.

For simplicity of notation, define:

$$g(w) \equiv \int_{1}^{w} \frac{\theta}{\theta_m} u^+ \, (1 - y/R) \, d \, (y/R) \qquad \text{(IV-4)}$$

Equation (IV-3) can now be rearranged and integrated a second time with respect to the radius ratio, w, to become:

$$R^2 u^* \frac{\theta_c}{\theta_m} \frac{\partial \theta_m}{\partial x} \frac{1}{\sigma \nu} \int_{1}^{z} \frac{g(w) \, dw}{(1 - w)\left[\frac{\alpha + \epsilon_H}{\sigma \nu}\right]} = \theta - \theta_c \qquad \text{(IV-5)}$$

where $1 \geq z \geq 0$.

Substitutions of Equations (III-11) and (III-25) into Equation (IV-5) yields:

$$R^2 u^* \frac{\theta_c}{\theta_m} \frac{\partial \theta_m}{\partial x} \frac{1}{\sigma \nu} G(z) = \theta - \theta_c \qquad \text{(IV-6)}$$

Where, again, for simplicity, define:

$$G(z) \equiv \int_{1}^{z} \frac{g(w) \, dw}{(1 - w)\left[\frac{Re^*(1-w)}{2 \, du^+/dw} - 1 + \frac{1}{\sigma Pr}\right]} \qquad \text{(IV-7)}$$

where $1 \geq z \geq 0$.

Also Equation (IV-3) when integrated over the entire region from z = 1 to z = 0 becomes:

$$R^2 u^* \frac{\theta_c}{\theta_m} \frac{\partial \theta_m}{\partial x} \frac{1}{\sigma \nu} G(0) = - \theta_c \qquad \text{(IV-8)}$$

Thus, dividing Equation (IV-6) by Equation (IV-8), an expression for the generalized temperature distribution can be obtained in the form:

$$\frac{\theta}{\theta_c} = 1 - \frac{\theta - \theta_c}{-\theta_c} = 1 - \frac{G(z)}{G(0)} \qquad \text{(IV-9)}$$

An equation for the heat flow in round pipe can be expressed in terms of θ as:

$$\pi D h \theta_m = -\frac{\pi D^2}{4} \rho C_p \bar{u} \frac{\partial \theta_m}{\partial x} \qquad \text{(IV-10)}$$

which can be written in the form:

$$Nu = \frac{hD}{\alpha \rho C_p} z - \frac{D^2}{4} \frac{1}{\theta_m} \frac{\partial \theta_m}{\partial x} \frac{\bar{u}}{\alpha} \qquad \text{(IV-11)}$$

Now Equation (IV-8) can be rearranged to the form:

$$\frac{D^2}{4} \frac{1}{\theta_m} \frac{\partial \theta_m}{\partial x} u^* = -\frac{\sigma \nu}{G(0)} \qquad \text{(IV-12)}$$

Substituting Equation (III-19) into Equation (IV-12) and combining the resulting equation with Equation (IV-11) yields:

$$Nu = -\frac{D^2}{4} \frac{1}{\alpha \theta_m} \frac{\partial \theta_m}{\partial x} \bar{u} \qquad \text{(IV-13)}$$

or

$$Nu = \frac{\sigma Pr}{\lambda} \frac{1}{G(0)} \qquad \text{(IV-14)}$$

As was the case for Chapter III, the introduction of Equations (II-12) and (II-14) into Equations (IV-4) and (IV-7) in the appropriate regions yields equations for the temperature distribution and heat transfer coefficient for the system.

Region of Fully Developed Turbulence

$$g_1(w) = \int_0^w \frac{\theta}{\theta_m} \{4.0986 + 2.778 \ln Re^* - \frac{1}{\ln Re^* - 7} + (2.7660 + 0.00125 \ln Re^*) [\ln(y/R) - 0.1 (y/R)^{10}]\} \times (1 - y/R)\, d(y/R) \qquad \text{(IV-15)}$$

where $1 \geq w \geq 70/Re^*$.

$$G(z) = \int_1^z \frac{g_1(w)\, dw}{(1-w)\left[\frac{Re^* w(1-w)}{(5.532+0.0052 \ln Re^*)(1-w^{10})} + 1 + \frac{1}{Pr}\right]} \qquad \text{(IV-16)}$$

where $1 \geq z \geq 70/Re^*$.

Region Adjacent to the Pipe Wall

$$g_2(w) = \int_{70/Re^*}^w \frac{\theta}{\theta_m} (1 - y/R) \times \left\{ \int_{70/Re^*}^{y/R} \frac{Re^* (1 - y/R)\, d(y/R)}{1+\{1+0.016(1-y/R)(Re^* y/R)^2 [1-\exp(-\frac{Re^* y/R}{54})]^2\}^{1/2}} \right\} d(y/R) \qquad \text{(IV-17)}$$

where $70/Re^* \geq w \geq 0$.

$$G(w) = \int_{70/Re^*}^{z} \frac{g_1(w) + g_2(w)\, dw}{(1-w)\left[\frac{Re^*(1-w)}{2+2\{1+0.016(1-2)(Re^*w)^2[1-\exp(-\frac{Re^*w}{54})]^2\}^{1/2}} - 1 + \frac{1}{Pr} \right]} \qquad \text{(IV-18)}$$

where $70/Re^* \geq z \geq 0$.

Equations (IV-16) and (IV-18) can thus be used in Equation (IV-9) to evaluate the radial temperature distribution. These equations are implicit in terms of θ, however, and must be solved by an iterative procedure in order to converge on the desired temperature distribution. Once the desired accuracy of the temperature distribution is obtained, Equation (IV-14) can be evaluated immediately for the heat transfer coefficient for the system under conditions of constant temperature at the pipe wall.

The results obtained here were calculated by use of the previously mentioned digital computer employing the above iterative procedure. The integrations involved were accomplished by utilizing the trapezoidal rule with fifty intervals being taken in the region of fully developed turbulence and thirty intervals in the region adjacent to the pipe wall. A linear temperature distribution was assumed as a first approximation with iterations being continued until two successive values of the Nusselt number differed by less than 0.005. Generally, six or seven iterations were required for sufficient convergence.

As a test of computational accuracy several values were recomputed utilizing eighty and fifty intervals in the two regions, respectively, and ten iterations were performed. In all cases tested the computed values differed by less than 0.5 per cent.

CHAPTER V

DISCUSSION OF RESULTS

The solution of the energy equation of the system under consideration, Equation (III-1), for the temperature distribution and heat transfer coefficient of a fluid in turbulent motion is contingent upon a knowledge of the velocity distribution and eddy diffusivity of heat transfer for the fluid. In momentum-heat transfer analogy techniques, this eddy diffusivity is in turn contingent upon a knowledge of the eddy diffusivity of momentum and the parameter $\sigma \equiv \epsilon_H/\epsilon_m$.

In addition to the above theoretical considerations which must be appraised in momentum-heat transfer analogy models, there are several postulates in the "ideal" heat transfer case that might not be duplicated in an actual engineering situation and which, therefore, must be considered. For example, most analogy models are developed for flow in smooth pipe whereas this situation rarely arises in practice; analogy models also postulate no axial conduction which, under certain conditions for liquid metals, is not a valid assumption; and no allowance is made for gas entrainment or pipe wall "wetting" effects. The following paragraphs will be devoted to discussion of some of these questions.

Once the eddy diffusivity of momentum is obtained from the momentum equation of the system and an appropriate velocity distribution equation, the eddy diffusivity of heat transfer can be obtained from the equation $\sigma \equiv \epsilon_H/\epsilon_m$, if σ is known. The ratio of the eddy diffusivities,

σ, has been described as the "true measure of our ignorance of the mechanism of heat transfer in turbulent motion." (27) Reichardt (11) postulates that $1 < \sigma < 2$. Jenkins (28) proposed a modification to Prandtl's mixing length theory to account for the loss of heat and momentum during the time the eddy is displaced. His theory predicts values of σ greater than one for fluids with Prandtl numbers greater than one and values of σ less than one for Prandtl numbers less than one. The extensive studies of air conducted by Sage, et al.,(29), (30), and (31), indicate that σ is greater than one. Isakoff and Drew (24) report values ranging up to approximately $\sigma = 1.7$ for mercury. Brown, et al., (32), report values of mercury ranging up to approximately $\sigma = 0.95$.

The actual value of the ratio of the eddies is probably not a constant but a function of several variables including Reynolds number, Prandtl number, roughness of the pipe wall and position within the pipe. In this analysis, σ has been included in the development as an unknown constant. If the ratio of the eddies can be accurately expressed by some mean value for the system, the equations developed in Chapters III and IV are exact for a system obeying the postulates as stated. It is interesting to note that in all equations developed in Chapters III and IV for the temperature distribution and heat transfer coefficient, the parameter σ always appears in a product with the Prandtl number. Hence, if one defines a pseudo Prandtl number $Pr' \equiv \sigma Pr$, all the σ's can be eliminated from the equations for the temperature distribution and heat transfer coefficient.

It was pointed out that a value of unity has been selected for σ in the numerical evaluation of the equations of this study. If subsequent

study reveals the mean value of σ should be different from unity, the results of this study can be easily corrected by use of a pseudo Prandtl number for the system obtained from the equation $Pr' = \sigma Pr$. Fig. 4 illustrates the effect of σ upon the heat transfer coefficient of the system.

The radial velocity distribution of the fluid has been discussed in Chapter II. It is the opinion of this writer that Equations (II-12) and (II-14) accurately express the velocity of a fluid as a function of radial position for isothermal flow in smooth circular pipes. For any actual heat transfer system, however, the flow is non-isothermal and the pipe will be rough to a certain degree. Franklet (18) in his model, based on the von Karman equations, considered the case of rough pipe and concluded that the heat transfer coefficient of liquid metals is increased from six to twelve per cent depending upon the roughness of the pipe.

In this study the data of Nikuradse (33) for rough pipe was examined and it was found that the constants in the velocity distribution equation, Equation (II-12), would be altered for rough pipe. Nikuradse's data are not accurate near the pipe wall so that the conclusions as to the effect of roughness on the velocity distribution and, hence, on the temperature distribution and heat transfer coefficient for the system could only be considered qualitatively. Investigation indicated an increase in the heat transfer coefficient of up to ten to fifteen per cent for fluids with Prandtl numbers less than 0.5 and an increase of up to three to ten per cent for fluids with Prandtl numbers greater than 0.5.

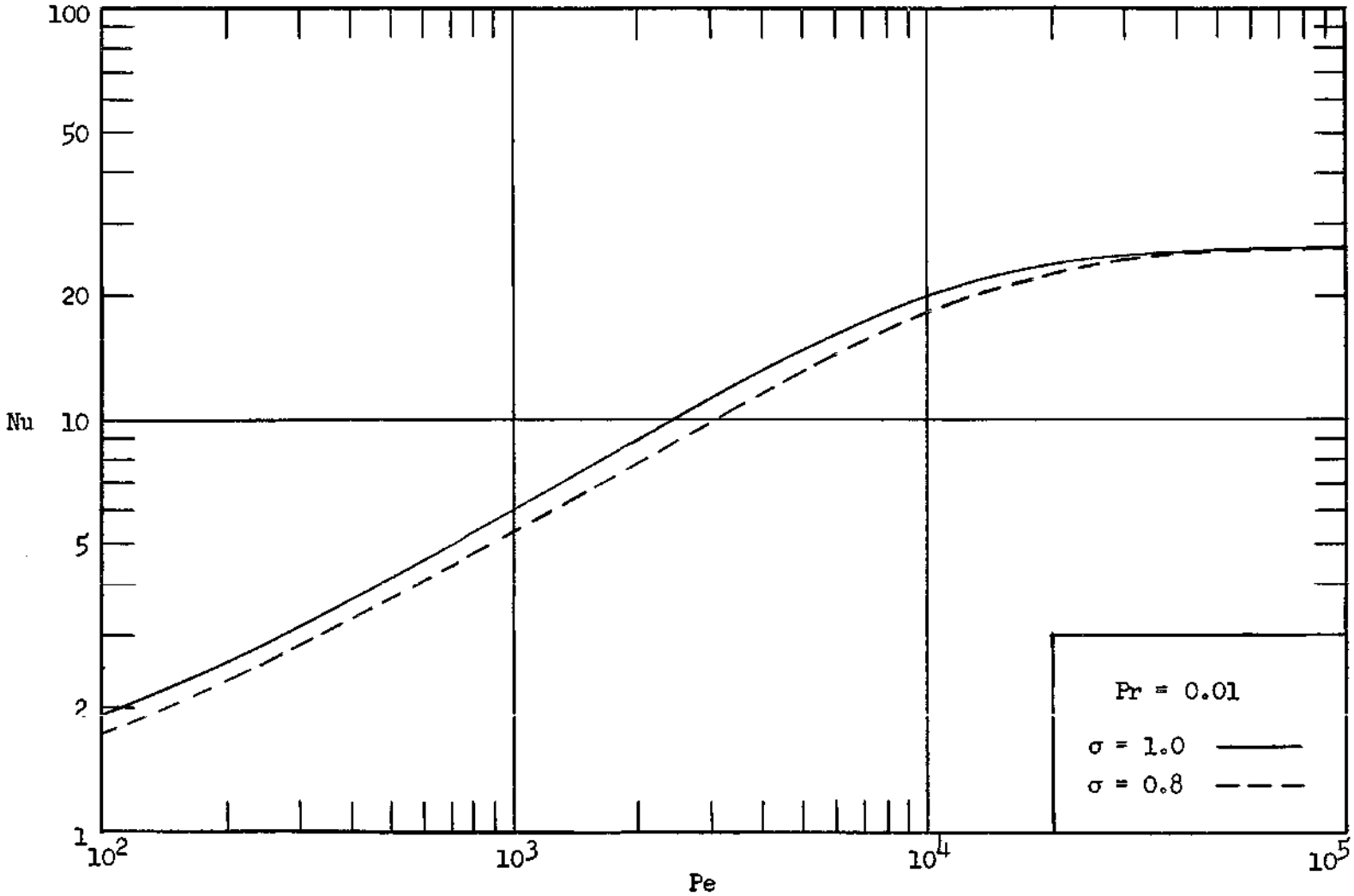

Figure 4. Nusselt Number as a Function of Peclet Number and the Ratio of Diffusivities of Heat and Momentum

There are insufficient data available to quantitatively consider the effect of non-isothermal temperature distributions upon the velocity distribution of the system. The meager data available do indicate, however, that the velocity distribution is affected only insofar as the viscosity of the fluid is affected by temperature changes. For the vast majority of fluids, the viscosity can be assumed constant over moderate ranges of temperature and, therefore, it can be assumed that the error introduced in the heat transfer coefficient by employing isothermal velocity distribution equations is negligible for most fluids.

Pipe wall "wetting" effects and gas entrainment are two additional phenomena which can take place in a practical heat transfer system which are not considered in the analytical model as presented. MacDonald and Quittenton (34) have considered these effects and conclude that a fluid which does not "wet" the pipe wall can have a heat transfer coefficient considerably different from that predicted by the analytical model. Since the heat transfer coefficient is lower for a non-wetting fluid than would be expected, systems employing such fluids normally have a "wetting" agent added to improve the heat transfer characteristics. When this is done the experimental heat transfer coefficient falls within the range of those predicted by the analogy model as presented.

Hoffman, Chelemer, Stansbury and Boarts (35) have analyzed the effect of gas entrainment and conclude that the heat transfer coefficient of a liquid with entrained gas will be lower than that of the same liquid with no entrained gas. The amount of this lowering, however, is considerably in doubt. Minute quantities of gas can affect the heat transfer coefficient greatly if the pockets of entrained gas occur as extended

planes or gaps. The same quantity of gas occurring in the form of small spherical bubbles would have a minor effect on the heat transfer coefficient. In view of the turbulence which exists within the system, the latter case appears more feasible in a realistic situation. Therefore, unless large quantitites of gas are entrained in the liquid, it appears that gas entrainment should not affect the heat transfer coefficient very greatly.

It has been assumed in the derivation of the energy equation for the system that the molecular and eddy transfer of heat is negligible in the axial direction compared to that in the radial direction. For fluids with Prandtl numbers greater than about 0.5 this assumption appears quite valid but for liquid metals it is questionable due to their high molecular conductivity. Trefethen (36) presents an analysis of the situation and concludes that the experimental data appear to demonstrate axial conduction for liquid metals. His semi-theoretical analysis has led to a correlation for the correction of heat transfer coefficient predictions due to axial conduction for systems with Peclet numbers less than 150. This correction has been applied to the results of this investigation and the results are compared with the uncorrected values in Table 3.

Figure 5 shows the effect of Prandtl number on the temperature distribution for a constant Reynolds number. It can be seen that as the Prandtl number increases the temperature at any point within the pipe increases relative to the center line temperature. As a result the mean temperature across the pipe increases with increasing Prandtl number. For fluids with large Prandtl number, the change in temperature between

Table 3. Correction for Axial Conduction

Applied to Nusselt Numbers

Pr	Re	Pe	Nu Uncorrected	Nu Corrected
0.01	5,000	50	1.67	1.29
			3.19	2.48
0.01	10,000	100	2.06	1.91
			3.62	3.35
0.02	5,000	100	3.39	3.05
			5.96	5.45

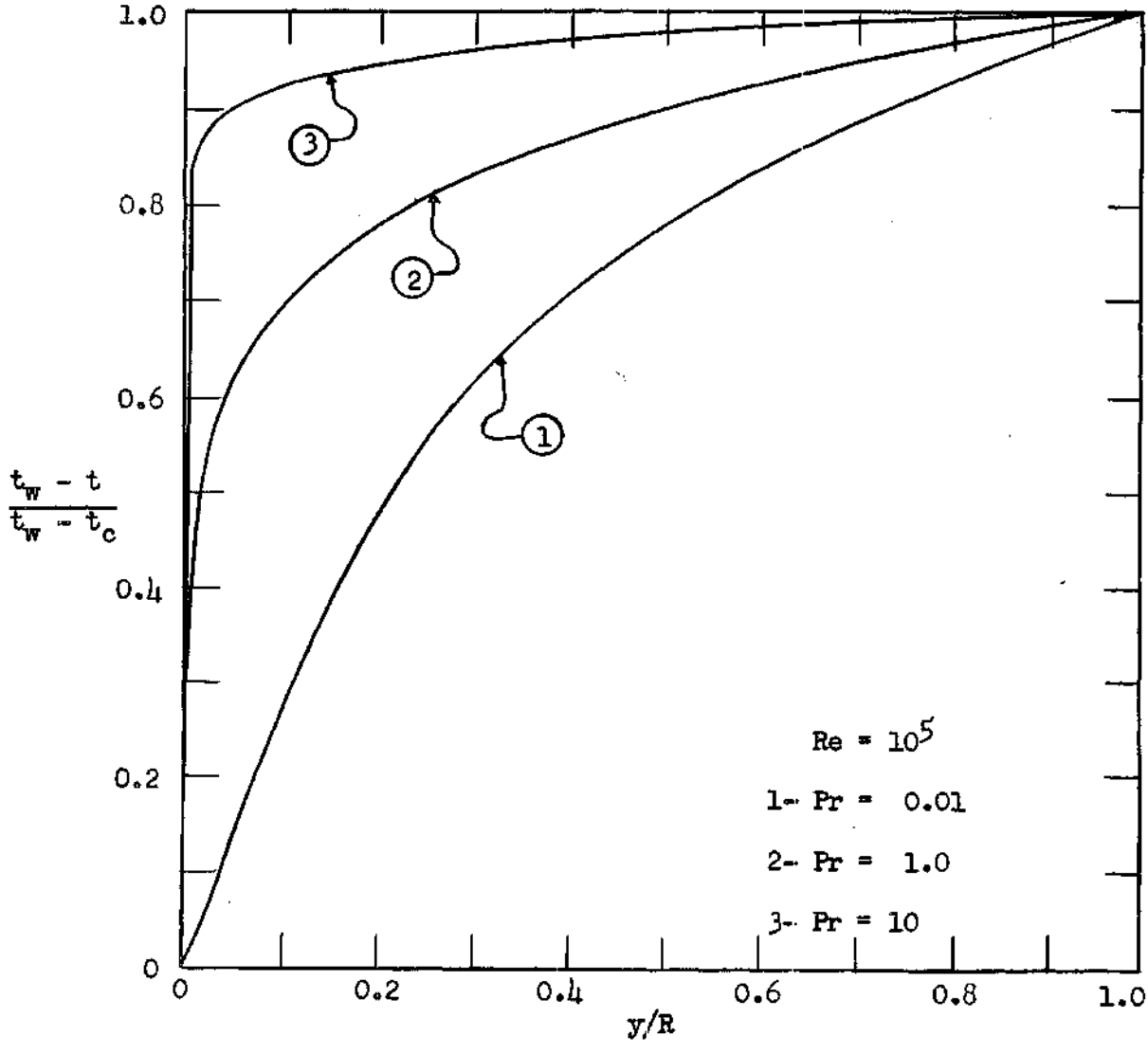

Figure 5. Temperature Distribution as a Function of Prandtl Number

the wall and the fluid is localized in the region immediately adjacent to the pipe wall, and the temperature is almost constant across the remainder of the pipe. Thus the magnitude of the mean temperature of the fluid is insignificantly affected by variation in the temperature of the wall.

Figure 6 shows the effect of Reynolds number on the temperature distribution for constant Prandtl number. Here again the temperature at any point increases relative to the center line temperature for increasing Reynolds number. Thus for sufficiently large Reynolds number the mean temperature is essentially independent of variations in the wall temperature and becomes approximately equal to the center line temperature regardless of the Prandtl number.

The difference in temperature distributions indicated for the case of constant heat flux at the pipe wall as compared to the case of constant temperature at the pipe wall is shown in Fig. 7. It can be seen that for the same wall to center line temperature difference the heat transfer rate is less for the case of constant wall temperature. This does not exactly reflect the difference in the heat transfer coefficients, since the mean temperature magnitudes are also different for the two cases.

Table 4 lists the values for the heat transfer coefficient expressed as Nusselt number as calculated in this investigation for both constant heat flux and constant temperature at the pipe wall. It also lists a comparison of these values expressed as a ratio of the Nusselt numbers for the two cases. From this table it can be seen that as Prandtl number increases the ratio of the Nusselt number for the two systems tends to

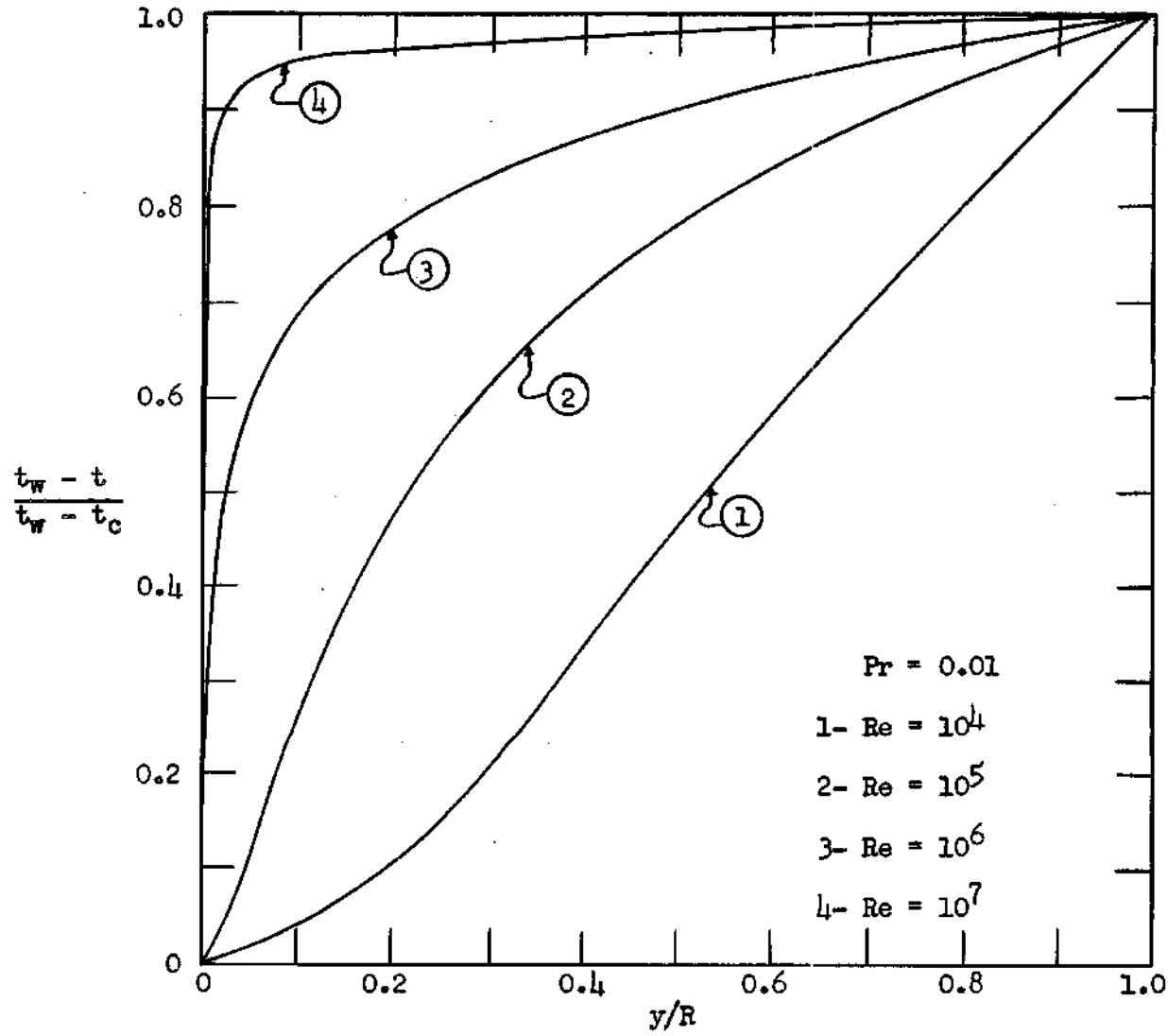

Figure 6. Temperature Distribution as a Function of Reynolds Number

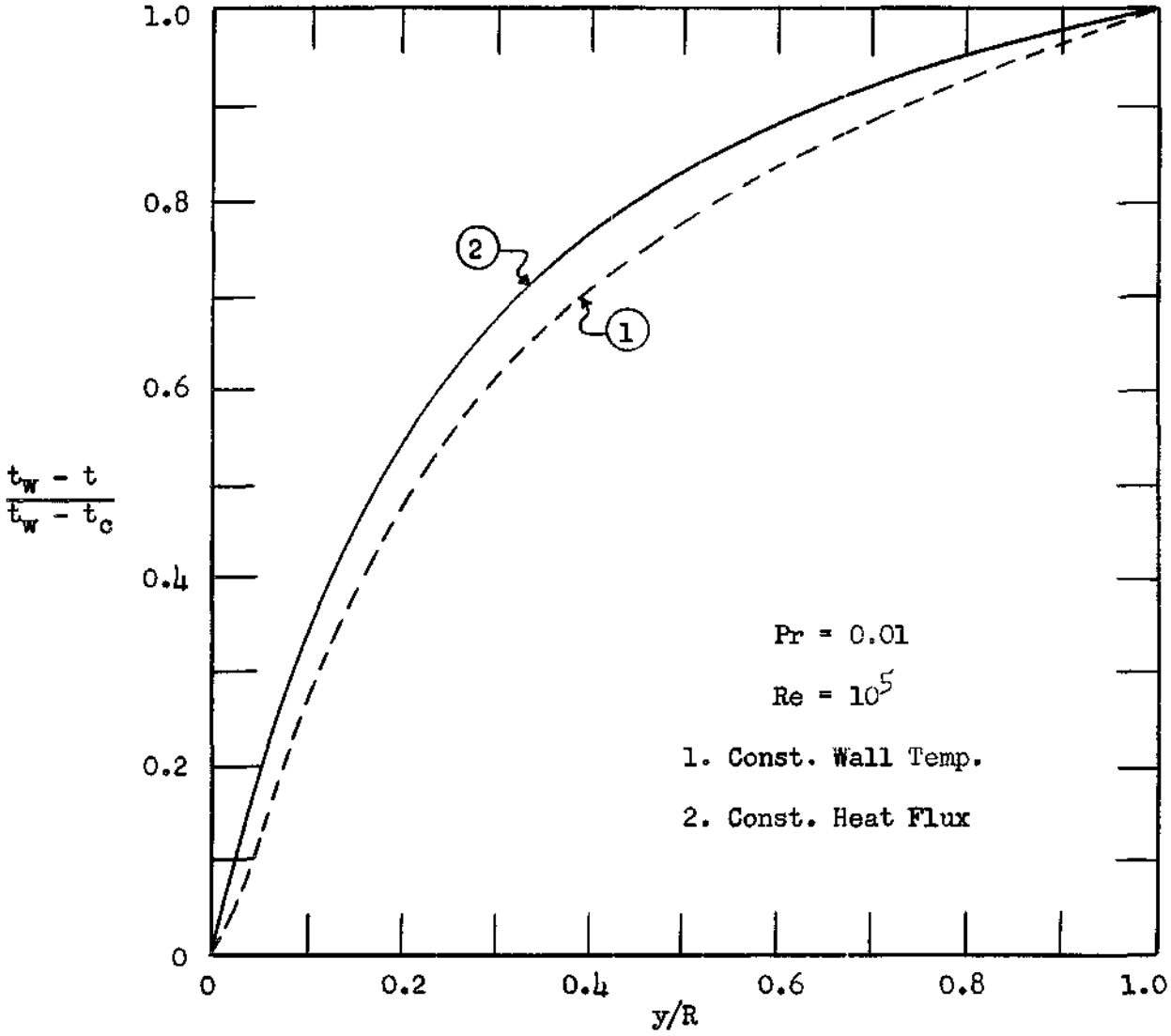

Figure 7. Temperature Distribution of Constant Wall Temperature and Constant Heat Flux

Table 4. Calculated Values of Nusselt Number

Pr	Re	Pe	Nu_q q_w Const.	Nu_t t_w Const.	$\frac{(Nu)_t}{(Nu)_q}$
0.01	5,000	50	2.48	1.29	0.52
	10,000	100	3.35	1.91	0.57
	30,000	300	4.51	3.20	0.71
	100,000	1,000	7.42	5.93	0.80
	300,000	3,000	14.2	11.1	0.78
	1,000,000	10,000	32.8	19.8	0.60
	3,000,000	30,000	74.0	25.2	0.34
	10,000,000	100,000	190	26.1	0.14
0.02	5,000	100	5.45	3.05	0.56
	10,000	200	6.57	4.07	0.62
	30,000	600	7.91	5.85	0.74
	100,000	2,000	13.00	10.7	0.82
	300,000	6,000	27.1	21.7	0.80
	1,000,000	20,000	62.5	38.1	0.61
	3,000,000	60,000	144	53.3	0.37
	10,000,000	200,000	370	59.2	0.16
0.7	10,000	7,000	32.5	29.6	0.91
	30,000	21,000	71.4	67.1	0.94
	100,000	70,000	179	170	0.95
	300,000	210,000	422	397	0.94
	1,000,000	700,000	1,125	889	0.79
	3,000,000	2,100,000	2,820	1,610	0.57
	10,000,000	7,000,000	7,910	2,290	0.29

Table 4. Continued

Pr	Re	Pe	Nu_q q_w Const.	Nu_t t_w Const.	$\frac{(Nu)_t}{(Nu)_q}$
1.0	10,000	10,000	37.9	35.2	0.93
	30,000	30,000	90.8	86.3	0.95
	100,000	100,000	217	208	0.96
	300,000	300,000	515	489	0.95
	1,000,000	1,000,000	1,430	1,140	0.80
	3,000,000	3,000,000	3,590	2,080	0.58
	10,000,000	10,000,000	10,500	3,150	0.30
10	10,000	100,000	97.2	94.3	0.97
	30,000	300,000	239	232	0.97
	100,000	1,000,000	676	662	0.98
	300,000	3,000,000	1,730	1,680	0.97
	1,000,000	10,000,000	5,090	4,630	0.91
	3,000,000	30,000,000	13,300	9,840	0.74
	10,000,000	100,000,000	40,100	16,800	0.42
100	10,000	1,000,000	248	246	0.99
	30,000	3,000,000	635	629	0.99
	100,000	10,000,000	1,830	1,810	0.99
	300,000	30,000,000	4,880	4,780	0.98
	1,000,000	100,000,000	14,600	13,700	0.94
	3,000,000	300,000,000	38,300	30,600	0.80
	10,000,000	1,000,000,000	115,000	57,500	0.51

unity for any particular Reynolds number. It can also be seen that the ratio tends to unity with increasing Reynolds number less than about 300,000. For values of Reynolds number above 300,000, however, the difference between the Nusselt numbers for the two cases becomes greater for a particular value of Prandtl number. The comparison of the two systems is also shown graphically in Fig. 8.

In order to consider qualitatively the difference between the heat transfer coefficients for the two systems, Equation (IV-11) can be used to express the ratio of the coefficients under the same conditions of flow as

$$\frac{(Nu)_t}{(Nu)_q} = \frac{(t_m - t_w)_q}{(t_m - t_w)_t} \frac{(\partial t_m/\partial x)_t}{(\partial t_m/\partial x)_q} \qquad (V\text{-}1)$$

where the subscripts t and q refer to a system under conditions of constant wall temperature and constant heat flux respectively. For the case of constant heat flux, the term $\partial t_m/\partial x$ is constant for a particular system, whereas for the case of constant wall temperature $\partial t_m/\partial x$ is a function of Reynolds number and decreases with increasing Reynolds number. As stated above, for sufficiently large values of Reynolds number, the mean temperature is approximately equal to the center line temperature. Therefore, if the two systems are considered to have the same center line temperature, the heat transfer coefficients become a function of the axial mean temperature gradient. Thus the ratio of the heat transfer coefficients should decrease for sufficiently large Reynolds numbers. For low Prandtl numbers, however, at somewhat lower values of Reynolds number,

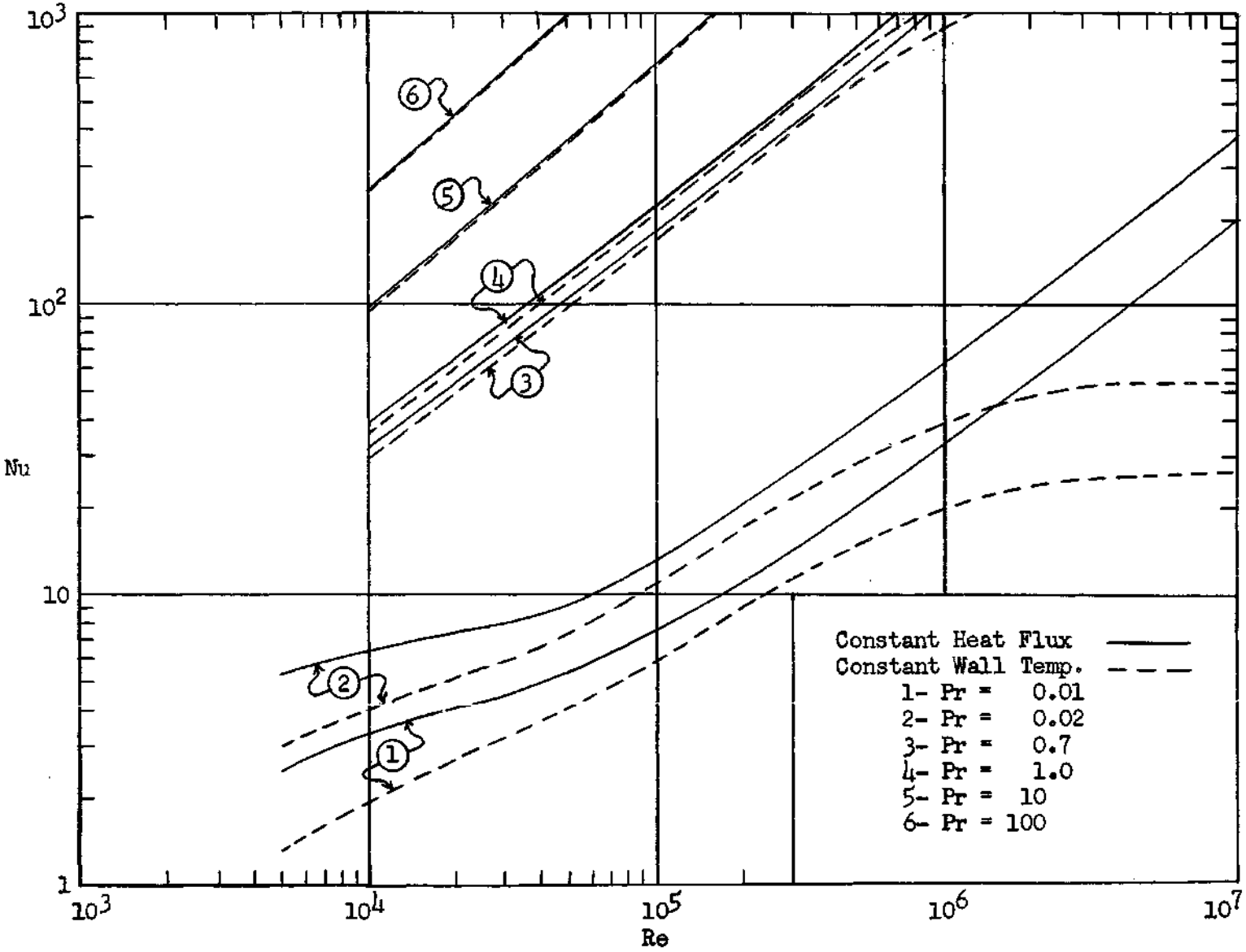

Figure 8. Nusselt Number as a Function of Reynolds Number and Prandtl Number

where the wall temperature affects the mean temperature appreciably, both the magnitude of the mean temperature gradient and the difference between the mean and wall temperatures becomes significant and it has been found that in this region the ratio of the heat transfer coefficients increases toward unity with increasing Prandtl number or Reynolds number. The ratios of the heat transfer coefficients computed in this investigation are shown graphically in Fig. 9.

An excellent review of the experimental investigations of liquids has been presented by Lubarsky and Kaufman (37). Subsequent investigations have been conducted by Chelemer (38); Mikheyev, Baum, Voskecensky and Fedynsky (39); Hall and Crofts (40); Kuczen and Bump (41); Brown, Amstead and Short (32); and Seban and Casey (42). Their results are in agreement with the bulk of the data as reviewed by Lubarsky and Kaufman except for the work of Brown, et al., which is higher. Fig. 10 presents the data, excluding those investigations which overlap the region as shown. The data for mercury have been re-evaluated using the thermal conductivity data of Ewing, Seebold, Grand and Miller (43).

Fig. 11 shows the predicted values of Nusselt number for Prandtl number values of 0.01 and 0.02 for the cases of both constant heat flux and constant wall temperature in comparison to the constant heat flux solution as computed by Martinelli (17) and with the experimental data shown in Fig. 10. The predicted values of Martinelli are plotted as originally reported along with the values corrected for axial conduction as applied in this investigation. Fig. 12 compares the heat transfer coefficient predicted for low Prandtly number fluids for the cases of

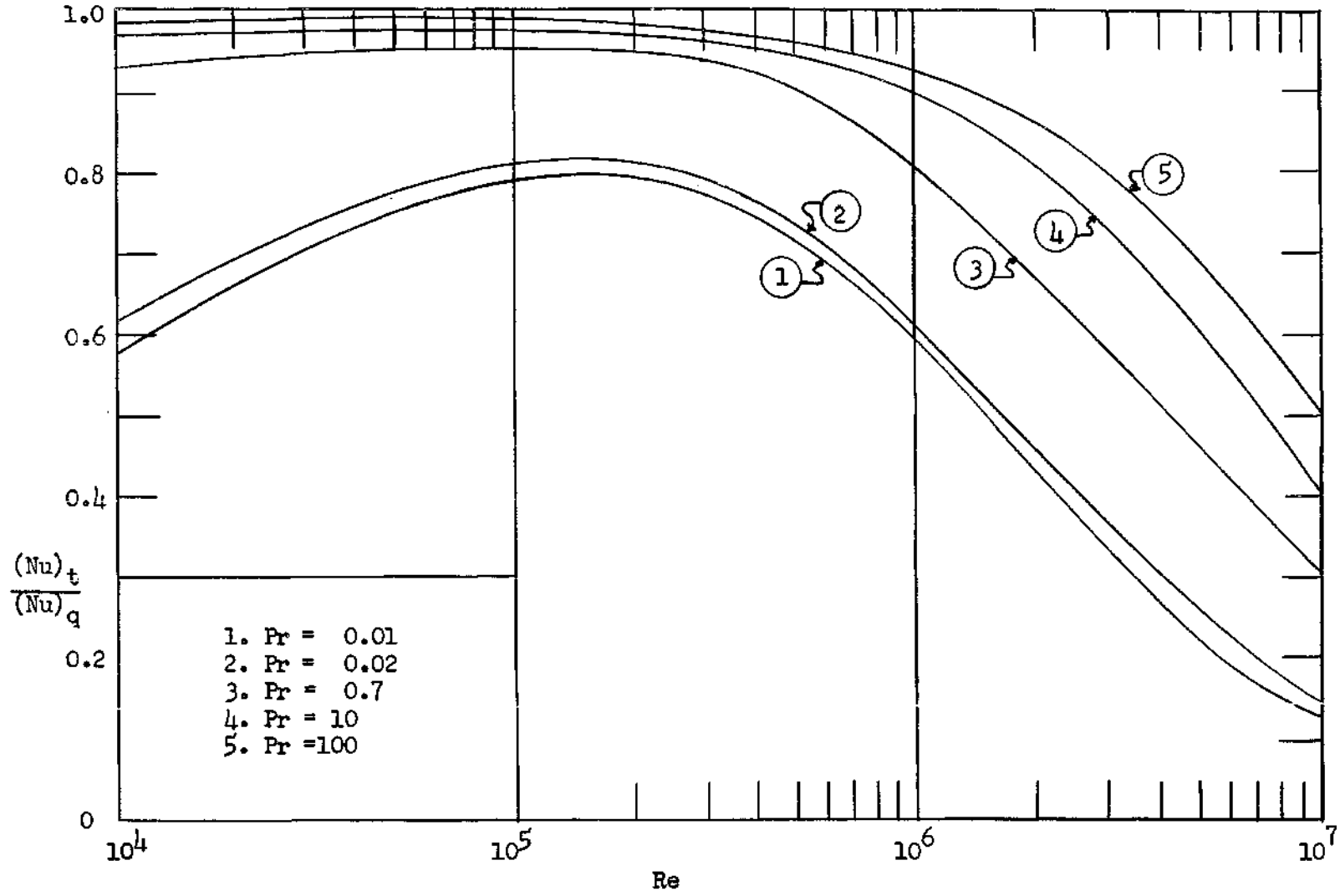

Figure 9. Ratio of Nusselt Numbers for Constant Wall Temperature to Constant Heat Flux as a Function of Reynolds Number and Prandtl Number

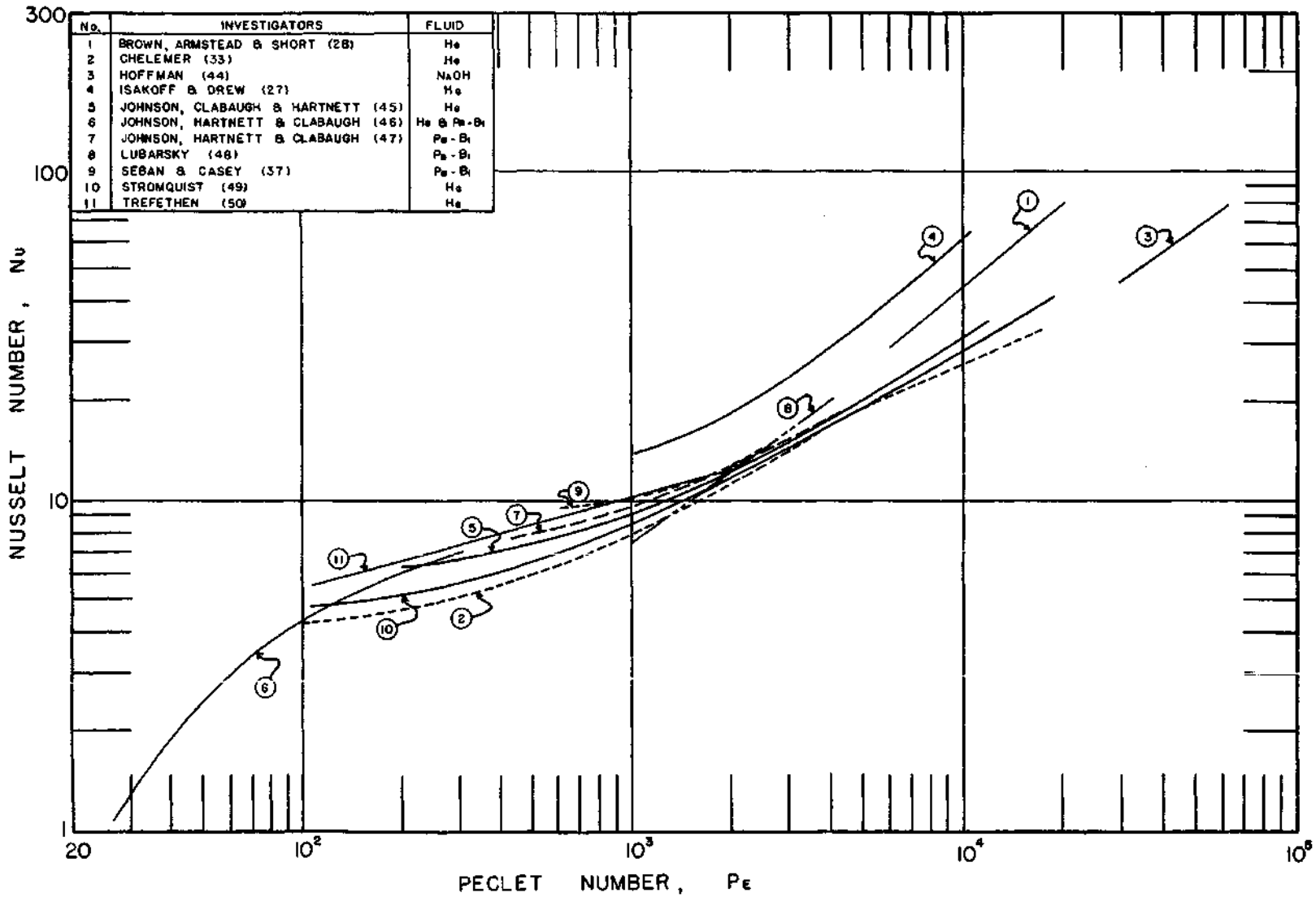

FIGURE 10. EXPERIMENTAL DATA

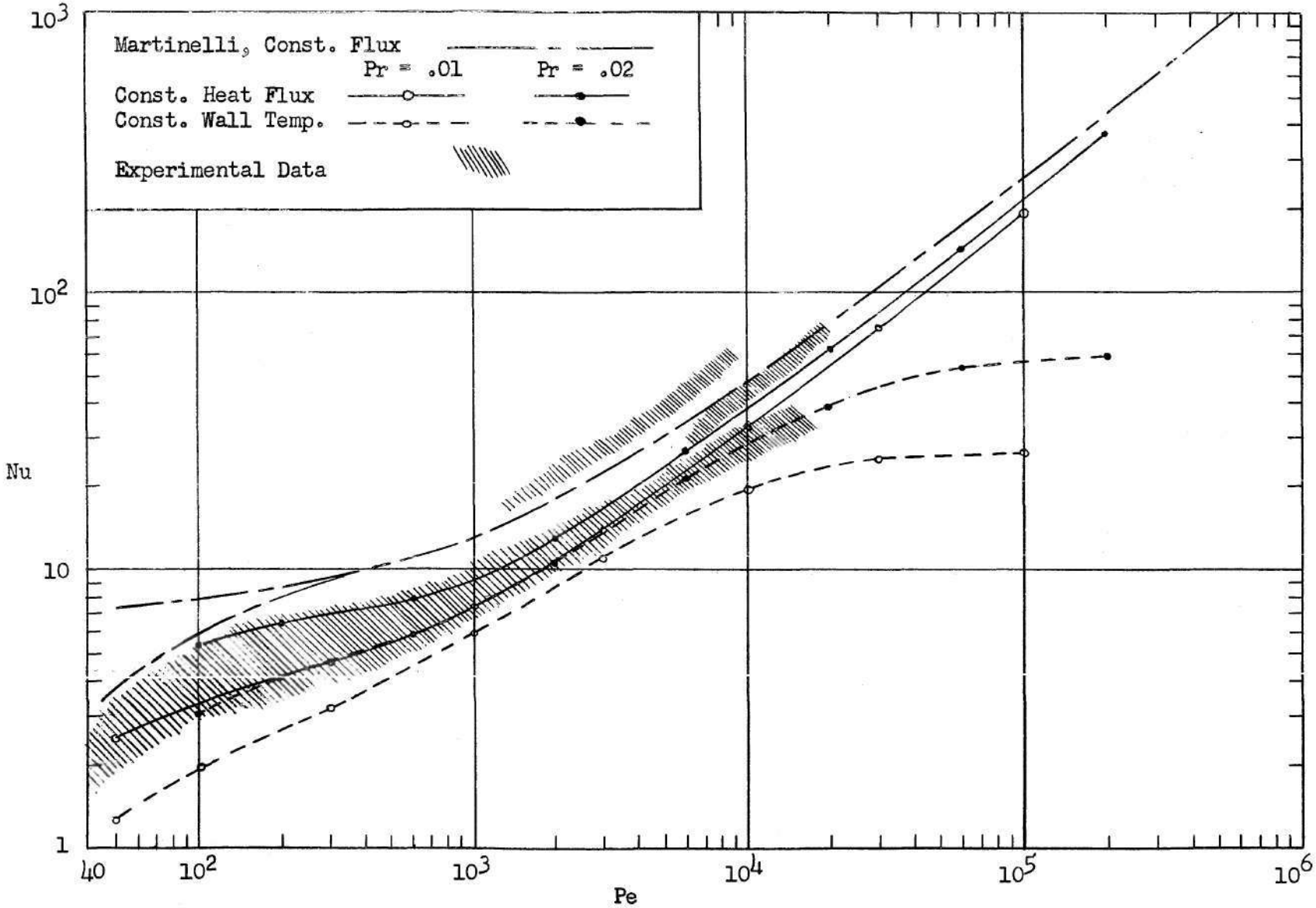

Figure 11. Nusselt Number as a Function of Peclet Number for Low Prandtl Numbers

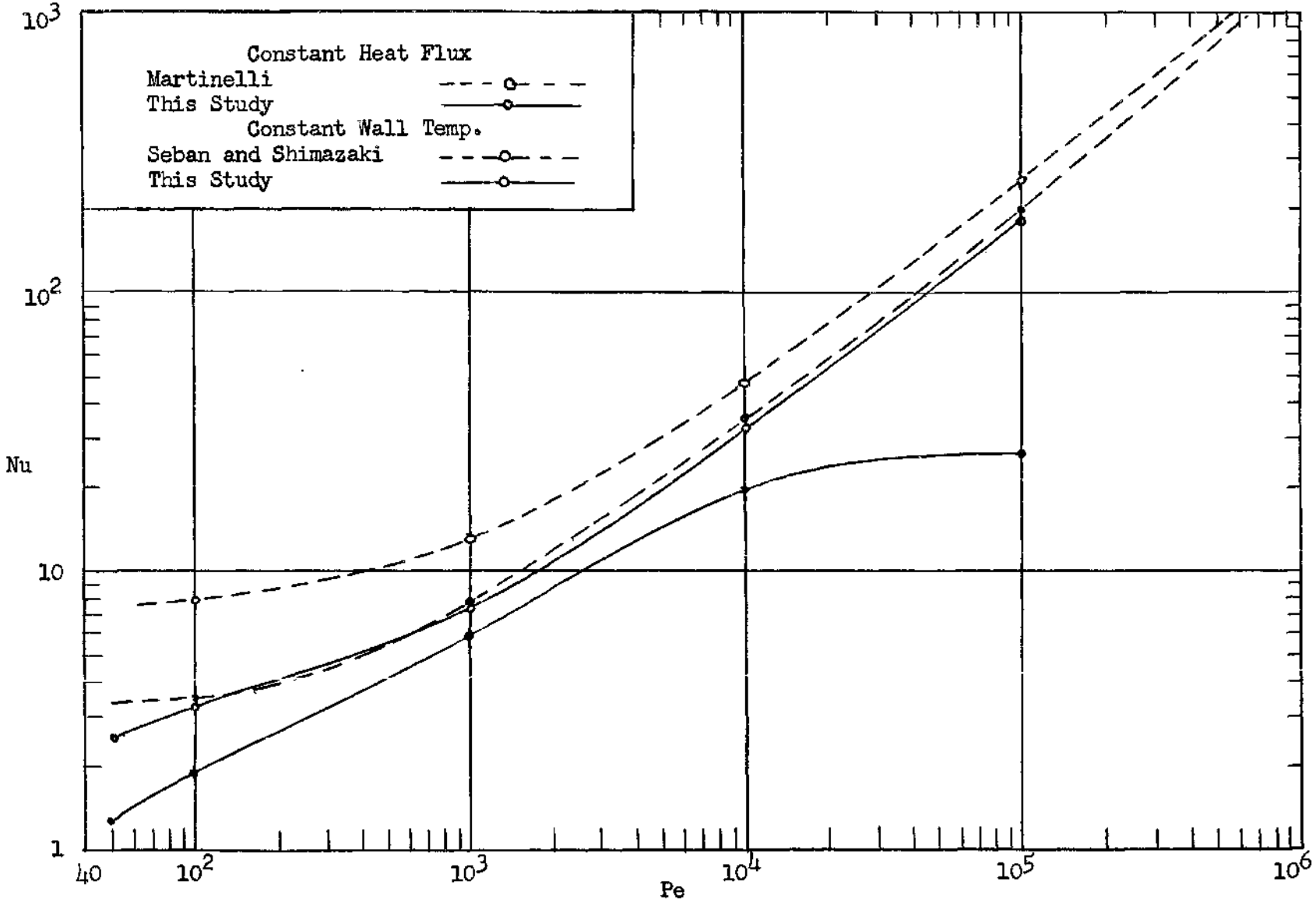

Figure 12. Predicted Values of Nusselt Number for low Prandtl Numbers

constant heat flux and constant wall temperature. The values computed in this investigation are compared with the predictions of Martinelli for constant heat flux and Seban and Shimazaki (13) for constant wall temperature.

Fig. 13 shows the predicted values of Nusselt numbers for Prandtl number values of 0.7, 1.0, 10 and 100 as compared to those predicted by Rannie (9). The predicted values of the heat transfer coefficient are compared to experimental data and Rannie's predictions for large Prandtl numbers in Fig. 14.

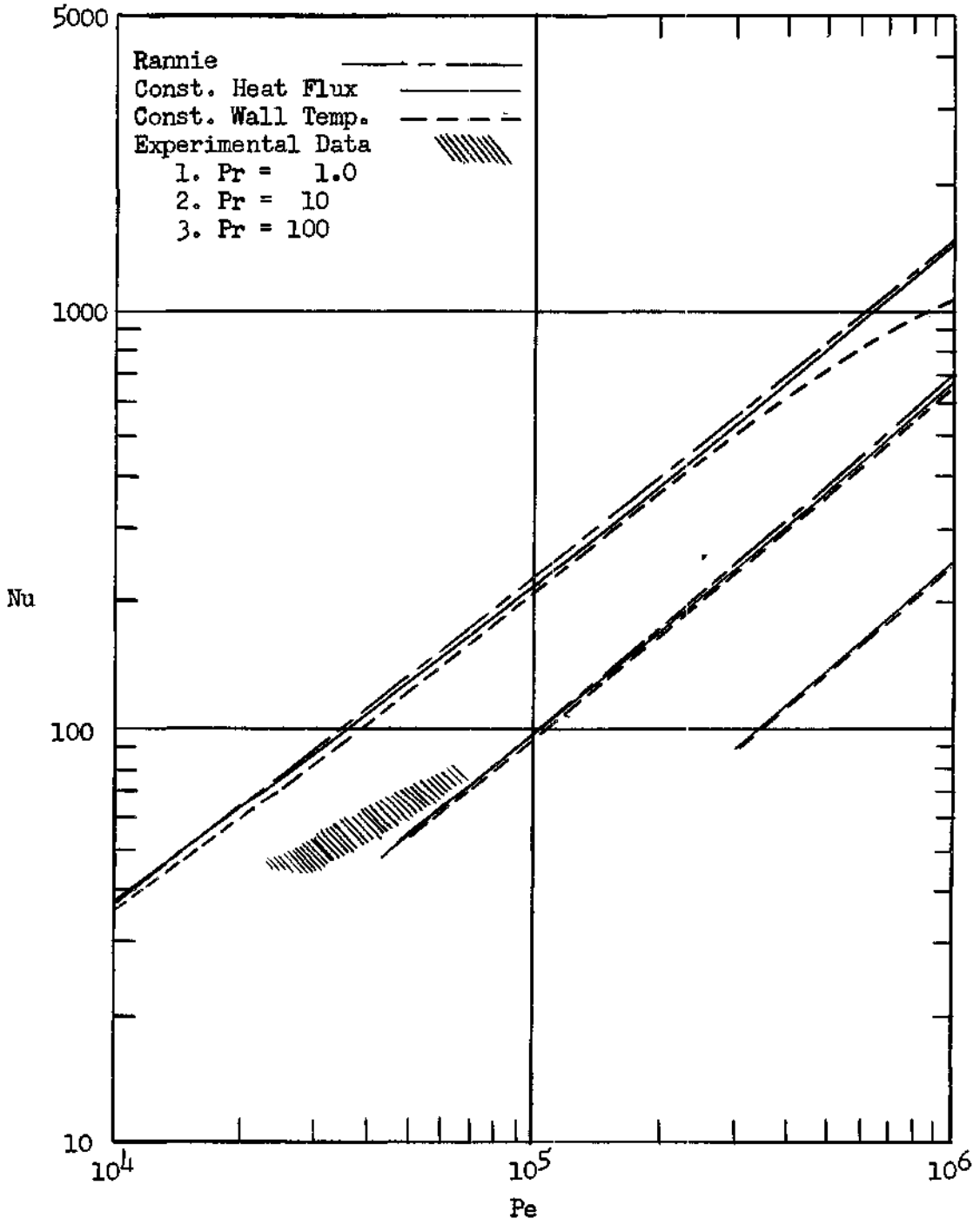

Figure 13. Nusselt Number as a Function of Peclet Number for Large Prandtl Numbers

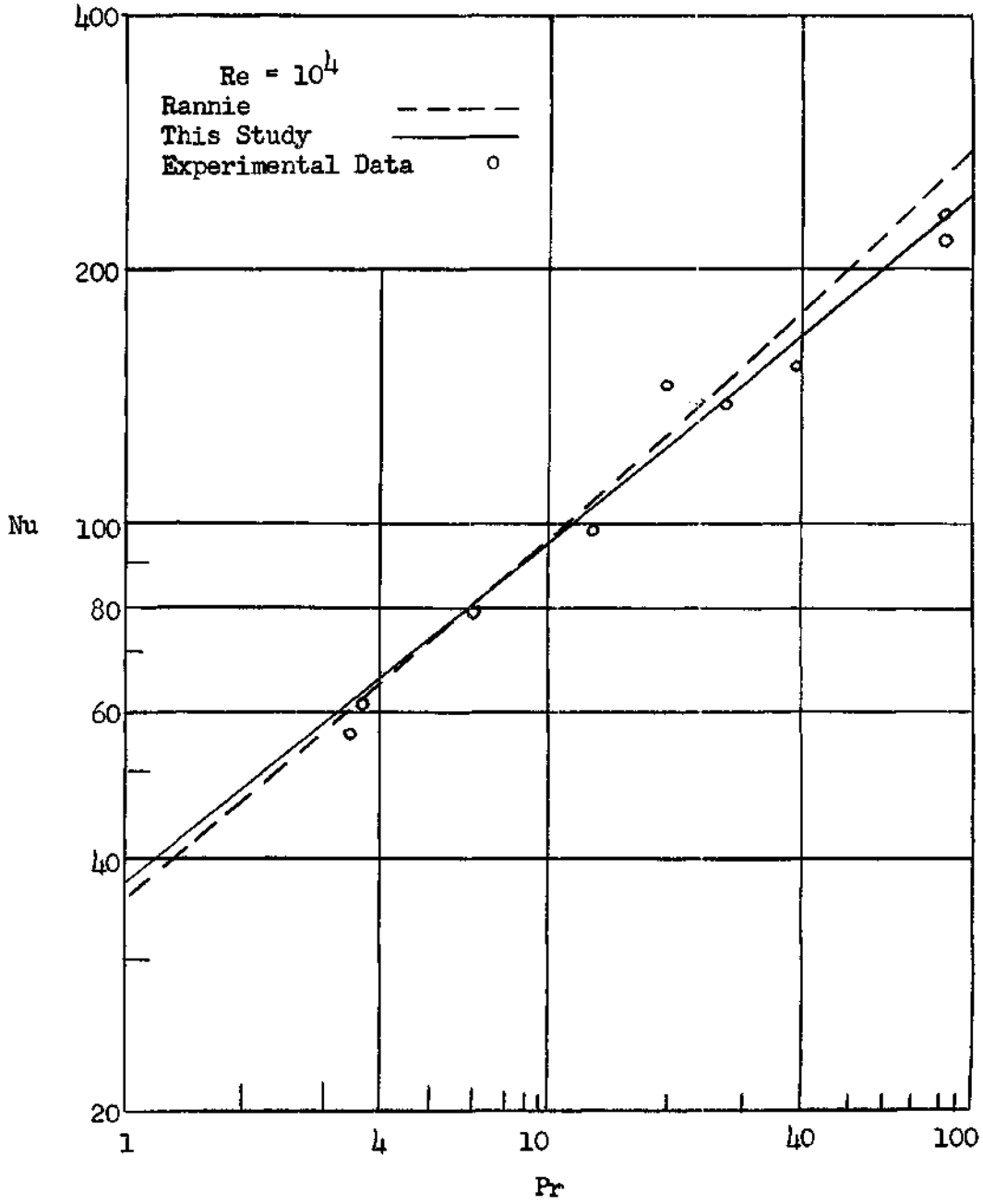

Figure 14. Predicted and Experimental Nusselt Numbers at Large Prandtl Numbers

CHAPTER VI

CONCLUSIONS AND RECOMMENDATIONS

An analytical model for the prediction of heat transfer coefficients of fluids in turbulent motion has been presented. This model is predicated upon an assumed relationship between the eddy diffusivities of momentum and heat and upon empirically developed velocity distribution equations. Based on the discussion presented in Chapter V, the following conclusions can be drawn as a result of this investigation.

1. Good agreement is obtained between the experimental heat transfer data and the predictions of this investigation over wide ranges of Reynolds number and Prandtl number.

2. The heat transfer coefficient of a fluid with Prandtl number greater than 0.5 is essentially independent of the temperature variation along the pipe wall over wide ranges of Reynolds number. This is not the case for fluids with very low Prandtl numbers, however. For such fluids it is found that the heat transfer coefficient may be as much as fifty per cent greater for the case of constant heat flux as it is for constant wall temperature.

3. The velocity distribution equation developed in the course of this investigation gives good agreement with experimental data and is in agreement with the theoretical knowledge of the velocity gradient.

The velocity distribution equation developed in this investigation is of such complexity that its use for simple velocity predictions, in

preference to the von Karman equations, is probably not justified. The primary contribution of this equation is its prediction of velocity gradients for which the von Karman equations are not accurate.

It is hoped that additional studies will encompass the following recommendations.

1. Ascertain experimentally the ratio of the eddy diffusivities of momentum and heat. The eddy diffusivities can be determined for any fluid from accurate velocity and temperature distribution measurements or they can be obtained more directly for gases by measuring the quantities $\overline{u'v'}$ and $\overline{u't'}$.

2. Determine the effect of pipe wall roughness on the velocity distribution within the pipe.

3. Determine the effect of non-isothermal temperature distributions on the velocity distribution within the pipe.

4. Explore more thoroughly the effects of axial conduction, gas entrainment and pipe wall "wetting" on the heat transfer coefficient of the system.

APPENDIX I

AXIAL TEMPERATURE DISTRIBUTION

CONSTANT WALL TEMPERATURE

In order to integrate the energy equation for the system defined in Chapter II, it is desirable to make use of the following lemma.

$$\frac{\partial}{\partial x}\left[\frac{t_w - \bar{t}}{t_w - t_m}\right] = 0 \tag{A-1}$$

This lemma can be verified for the system with a uniform wall temperature in the following manner. Consideration of a heat balance on a differential element of length dx yields

$$\frac{C_p \rho \bar{u} D}{4h} \frac{\partial t_m}{\partial x} = t_w - t_m \tag{A-2}$$

The mean radial temperature is defined by

$$t_m = \frac{\int_0^R \overline{\bar{t}\bar{u}} r dr}{\int_0^R \bar{u} r dr} \tag{A-3}$$

which when substituted into Equation (A-1) yields

$$\frac{C_p \rho \bar{u} D}{4h} \frac{\partial}{\partial x} \frac{\int_0^R \overline{\bar{t}\bar{u}} r dr}{\int_0^R \bar{u} r dr} = t_w - \frac{\int_0^R \overline{\bar{t}\bar{u}} r dr}{\int_0^R \bar{u} r dr} \tag{A-4}$$

Now $\bar{u}$ and r are independent of x and R is a constant, thus Equation (A-1) can be written as

$$\frac{C_p \rho \bar{u} D}{4h} \frac{\int_0^R \frac{\partial t}{\partial x} \bar{u} r dr}{\int_0^R \bar{u} r dr} = t_w - \frac{\int_0^R \overline{tu} r dr}{\int_0^R \bar{u} r dr} \qquad \text{(A-5)}$$

which when cleared of fractions becomes on differentiation

$$\frac{C_p \rho \bar{u} D}{4h} \frac{\partial \bar{t}}{\partial x} = t_w - \bar{t} \qquad \text{(A-6)}$$

Combining Equations (A-2) and (A-6), there is obtained

$$(t_w - \bar{t}) \frac{\partial t_m}{\partial x} - (t_w - t_m) \frac{\partial \bar{t}}{\partial x} = 0 \qquad \text{(A-7)}$$

Now since the wall temperature is constant

$$\frac{\partial (t_w - \bar{t})}{\partial x} = - \frac{\partial \bar{t}}{\partial x} \qquad \text{(A-8)}$$

and

$$\frac{\partial (t_w - t_m)}{\partial x} = - \frac{\partial t_m}{\partial x} \qquad \text{(A-9)}$$

Thus Equation (A-7) can be written as

$$(t_w - \bar{t}) \frac{\partial (t_w - t_m)}{\partial x} - (t_w - t_m) \frac{\partial (t_w - t_m)}{\partial x} \qquad \text{(A-10)}$$

By multiplying Equation (A-10) by $(t_w - t_m)^2/(t_w - t_m)^2$, it can be reduced to

$$(t_w - t_m)^2 \frac{\partial}{\partial x} \frac{t_w - \bar{t}}{t_w - t_m} = 0 \qquad \text{(A-11)}$$

Now since in general $t_w - t_m$ is not equal to zero it follows that

$$\frac{\partial}{\partial x} \left[\frac{t_w - \bar{t}}{t_w - t_m} \right] = 0 \qquad \text{(A-12)}$$

For the case of uniform wall temperature here considered Equation (A-12) reduces to

$$\frac{\partial t}{\partial x} = \frac{t_w - \bar{t}}{t_w - t_m} \frac{\partial t_m}{\partial x} \qquad \text{(A-13)}$$

or in terms of $\theta = t_w - \bar{t}$

$$\frac{\partial \theta}{\partial x} = \frac{\theta}{\theta_m} \frac{\partial \theta_m}{\partial x} \qquad \text{(A-14)}$$

BIBLIOGRAPHY

1. Summerfield, M., "Recent Developments in Convective Heat Transfer with Special Reference to High-Temperature Combustion Chambers," Heat Transfer Symposium, University of Michigan, 156-169 (1953).

2. Jakob, M., Heat Transfer, Vol. I, John Wiley and Sons, Inc., New York, 500-521 (1956).

3. Reichardt, H., "Heat Transfer Through Turbulent Friction Layers," National Advisory Committee for Aeronautics, Technical Note 1047, (1940).

4. Knudsen, J. G. and Katz, D. L., Fluid Dynamics and Heat Transfer, McGraw-Hill Book Company, Inc., New York, 407 (1958).

5. von Karman, T., Proceedings of the Fourth International Congress of Applied Mechanics, Cambridge, England, 1934.

6. Nikuradse, J., "Gesetzmassigkeiten der Turbulenten Stromung in Glatten Rohren," Vereinigung Deutschen Ingenieurn, Verlag G.M.B.H. (1932)

7. Deissler, R. G. and Eian, C. S., "Analytical and Experimental Investigation of Fully Developed Turbulent Flow in Air in a Smooth Tube with Heat Transfer with Variable Fluid Properties," National Advisory Committee for Aeronautics, Technical Note 2926 (1952).

8. Deissler, R. G., "Analysis of Turbulent Heat Transfer, Mass Transfer and Friction in Smooth Tubes at High Prandtl and Schmidt Numbers," National Advisory Committee for Aeronautics, Technical Note 3145 (1954).

9. Rannie, W. D., Heat Transfer in Turbulent Shear Flow, Ph.D. Thesis, California Institute of Technology (1951).

10. Reichardt, H., "Heat Transfer Through Turbulent Friction Layers," National Advisory Committee for Aeronautics, Technical Note 1047, (1940).

11. Reichardt, H., "The Principles of Turbulent Heat Transfer," National Advisory Committee for Aeronautics, Technical Ncte 1408 (1957).

12. van Driest, E. R., "On Turbulent Flow Near a Wall," Heat Transfer and Fluid Mechanics Institute, Paper No. XII, University of California (1955).

13. Seban, R. A., and Shimazaki, T. T., "Heat Transfer to a Fluid Flowing Turbulently in a Smooth Pipe with Walls at Constant Temperature," Transactions of the American Society of Mechanical Engineers 73, 803-808 (1951).

14. Hefner, R. J., Heat Transfer to Liquid Metals Flowing Turbulently in a Pipe with Walls at Constant Temperature, M.S. Thesis, Georgia Institute of Technology (1958).

15. Sleicher, C. A., Heat Transfer in a Pipe with Turbulent Flow and Arbitrary Wall-Temperature, Ph.D. Thesis, University of Michigan (1956). Also, Sleicher, C. A., Jr., and Tribus, M., "Heat Transfer in a Pipe with Turbulent Flow and Arbitrary Wall-Temperature Distribution," Transactions of the American Society of Mechanical Engineers 79, 789-797 (1957).

16. Tribus, M., and Klein, V., "Forced Convection from Non-isothermal Surfaces," Heat Transfer, A Symposium Held at the University of Michigan During 1952, Engineering Research Institute, University of Michigan, Ann Arbor, Michigan, 211-235 (1953).

17. Martinelli, R. C., "Heat Transfer to Molten Metals," Transactions of the American Society of Mechanical Engineers 69, 947-959 (1947).

18. Franklet, D. L., Heat Transfer to Liquid Metals, Ph.D. Thesis, Georgia Institute of Technology (1958).

19. Deissler, R. G., National Advisory Committee for Aeronautics, Technical Note 1210 (1955).

20. Willers, F. A., Practical Analysis, Dover Publications, Inc., New York (1948).

21. Hilderbrand, F. B., Introduction to Numerical Analysis, McGraw-Hill Book Company, Inc., New York (1956).

22. Kopal, Z., Numerical Analysis, John Wiley and Sons, Inc., New York (1955).

23. Pannel, J. R., British Aeronautical Research Committee, Report Memorandum 243 (1916).

24. Isakoff, S. E. and Drew, T. B., "Heat and Momentum Transfer in Turbulent Flow of Mercury," Proceedings of the General Discussion on Heat Transfer, Institution of Mechanical Engineers, London, 405-409, and American Society of Mechanical Engineers, New York, 479-480. Also Isakoff, S. E., Heat and Momentum Transfer in Turbulent Flow of Mercury, Ph.D. Thesis, Columbia University (1952).

25. Weisberg, H. L., Velocity and Pressure Distributions in Turbulent Pipe Flow with Uniform Wall Suction, Ph.D. Thesis, University of Tennessee (1955).

26. Page, F.; Schlinger, W. G.; Breaux, D. K.; and Sage, B. H., Industrial Engineering Chemistry, 44, 424 (1952).

27. Lykoudis, P. S. and Touloukian, Y. S., "Heat Transfer in Liquid Metals," Transactions of the American Society of Mechanical Engineers 80, 653-666 (1958).

28. Jenkins, R., "Variation of the Eddy Conductivity with Prandtl Modulus and its Use in Prediction of Turbulent Heat Transfer Coefficients," 1951 Heat Transfer and Fluid Mechanics Institute, Stanford University (1951).

29. Page, F., Jr.; Schlinger, W. G.; Breaux, D. K.; and Sage, B. H., "Point Values of Eddy Conductivity and Viscosity in Uniform Flow Between Parallel Plates," Industrial and Engineering Chemistry 44, 428-430 (1952).

30. Schlinger, W. G.; Berry, V. J.; Mason, J. L.; and Sage, B. H., "Temperature Gradients in Turbulent Gas Streams," Industrial and Engineering Chemistry 45, 662-666 (1953).

31. Corcoran, W. H. and Sage, B. H., "Role of Eddy Conductivity in Thermal Transport," Journal of the American Institute of Chemical Engineers, 2, 251-258 (1956).

32. Brown, H. E.; Amstead, B. H.; and Short, B. E.,"Temperature and Velocity Distribution and Transfer of Heat in a Liquid Metal," Transactions of the American Society of Mechanical Engineers 79, 279-285 (1957).

33. Nikuradse, J., "Laws of Fluid Flow in Rough Pipes," Petroleum Engineer, March, May, June, July, August (1940).

34. MacDonald, N. C., and Quittenton, R. C., "A Critical Analysis of Metal 'Wetting' and Gas Entrainment in Heat Transfer to Molten Metals," American Institute of Chemical Engineers, Preprint No. 8 (1953).

35. Hoffman, B.; Chelemer, H.; Stansbury, E. E.; and Boarts, R. N., "The Effect of Entrainment on the Heat Transfer Characteristics of Liquid Mercury," Brookhaven National Laboratory 2446, 21-34 (1954).

36. Trefethen, L., "Measurement of Mean Fluid Temperatures," Transactions of the American Society of Mechanical Engineers 78, 1207-1212 (1956).

37. Lubarsky, B. and Kaufman, S. J., "Review of Experimental Investigations of Liquid-Metal Heat Transfer," National Advisory Committee for Aeronautics, Technical Note 3336 (1955).

38. Chelemer, Harold, Effect of Gas Entrainment on the Heat Transfer Characteristics of Mercury under Turbulent Flow Conditions, Ph.D. Thesis, University of Tennessee (1955).

39. Mikheyev, M. A.; Baum, V. A.; Voskerensky, K. D.; and Fedynsky, O. S., "Heat Transfer of Molten Metals," Proceedings of the International Conference on the Peaceful Uses of Atomic Energy (Geneva) 9, 285-289 (1956).

40. Hall, W. B. and Crofts, T. I. M., "The Use of Sodium and Sodium-Potassium Alloy as a Heat Transfer Medium," Atomics Engineering and Technology 7, 167-172, 271-273, 290 (1956).

41. Kuczen, K. D., and Bump, T. R., "Measurement of Local Heat Transfer Coefficients with Sodium-Potassium Eutectic in Turbulent Flow," Nuclear Science and Engineering 2, 181-199 (1957).

42. Seban, R. A. and Casey, D. E., "Heat Transfer to Lead-Bismuth in Turbulent Flow in an Annulus," Transactions of the American Society of Mechanical Engineers 79, 1514-1518 (1957).

43. Drew, T. B.; Koo, E. C.; and McAdams, W. H., "The Friction Factor for Clean Round Pipe," Transactions of the American Institute of Chemical Engineers 28, 56-72 (1932).

44. Hoffman, H. W., "Turbulent Forced Convection Heat Transfer in Circular Tubes Containing Molten Sodium Hydroxide," Oak Ridge National Laboratory 1370 (1952).

45. Johnson, H. A.; Clabaugh, W. J.; and Hartnett, J. P., "Heat Transfer to Mercury in Turbulent Pipe Flow," Report of the U. S. Atomic Energy Commission, Contract AT-11-1-GEN 10, Project 5, Phase II (1953).

46. Johnson, H. A.; Hartnett, J. P.; and Clabaugh, W. J., "Heat Transfer to Molten Lead-Bismuth Eutectic in Turbulent Pipe Flow," Final Report for the U. S. Atomic Energy Commission Research, Contract No. AT-(40-1)-1061, Part 2 (1951).

47. Johnson, H. A.; Hartnett, J. P.; and Clabaugh, W. J., "Heat Transfer to Lead-Bismuth and Mercury in Laminar and Transi-Pipe Flow," Report for the U. S. Atomic Energy Commission Research, Contract AT-11-1-GEN 10, Project 5, Phase II (1953).

48. Lubarsky, B., "Experimental Investigation of Forced-Convection Heat-Transfer Characteristics of Lead-Bismuth Eutectic," National Advisory Committee for Aeronautics, Report Memorandum E51G02 (1951).

49. Stromquist, W. K., Effect of Wetting on Heat Transfer Characteristics of Liquid Metals, Ph.D. Thesis, University of Tennessee (1953).

50. Trefethen, L. M., Heat Transfer Properties of Liquid Metals, NP-1788 Technical Information Service, U. S. Atomic Energy Commission, Oak Ridge (1950).

VITA

Robert J. Hefner was born in Gainesville, Georgia, on March 7, 1930. His wife is the former Miss Alice Orem of Norfolk, Virginia. He is the father of three daughters, Kathrine, Linda, and Patricia.

In the fall of 1948 he entered the Georgia Institute of Technology and received his bachelor's degree in Chemical Engineering in the spring of 1952. The ensuing three years were spent in the U. S. Navy, after which he returned to the Georgia Institute of Technology, where he received his Master's degree in Chemical Engineering in the spring of 1958. He is presently employed by the Union Carbide Corporation at the Oak Ridge National Laboratory, Oak Ridge, Tennessee.